[redacted]

Coordinated Science Laboratory

UNIVERSITY OF ILLINOIS - URBANA, ILLINOIS

MINIMIZATION OF ATMOSPHERIC TURBULENCE EFFECTS ON HIGH-RESOLUTION SYNTHETIC APERTURE SYSTEMS

Dale M. Diamond

REPORT R-179 SEPTEMBER, 1963

COORDINATED SCIENCE LABORATORY
UNIVERSITY OF ILLINOIS
URBANA, ILLINOIS

Contract DA-36-039-TR US AMC 02208(E)
DA Project 3A-99-25-004

The research reported in this document was made possible by support extended to the University of Illinois, Coordinated Science Laboratory, jointly by the Department of the Army, Department of the Navy (Office of Naval Research), and the Department of the Air Force (Office of Scientific Research) under Department of Army Contract DA-36-039-TR US AMC 02208(E).

ABSTRACT

A method of processing the received signals in a synthetic aperture radar system to remove the effects of atmospheric turbulence is proposed. An appropriate mathematical model of the synthetic system and the manner in which it is affected by atmospheric turbulence is developed. The model thus developed is used as the basis for a processing procedure which matches the first few terms of a Fourier series to the phase error effect caused by the atmospheric turbulence. Several examples of a computer simulation are used to illustrate the results of such processing.

ACKNOWLEDGMENT

The author is greatly indebted to Professor J. B. Cruz, Jr., whose advice and encouragement contributed greatly to the study reported here. Special appreciation is also extended to Professor D. L. Bitzer, who suggested the study and who contributed greatly through many helpful discussions. Appreciation is also extended to the members of the Coordinated Science Laboratory who, in one way or another, aided in the research reported here.

Thanks are also due to Mrs. Joann Gschwendtner, who typed the manuscript.

TABLE OF CONTENTS

LIST OF FIGURES

LIST OF FIGURES (Continued)

I. INTRODUCTION

Since the concept of the synthetic aperture radar system was first introduced by Carl Wiley of Goodyear Aircraft Corporation in June, 1951, considerable effort has been expended in developing it into an effective system. It is now recognized as a means of obtaining very high angular resolution in radar mapping or surveillance systems.[6] For a time there was no need to develop the synthetic system to its full capability, since there was no point in having better azimuth resolution than range resolution. With the advent of pulse compression techniques, however, better range resolution was obtainable and better performance was demanded of the synthetic system. It appears that the synthetic aperture system development is now approaching a limitation imposed by nature — atmospheric turbulence and its effect on antenna resolution.[1]

Variations in pressure, temperature, impurity content, vapor content, etc., associated with a turbulent atmosphere cause it to depart from homogeneity and results in a spatially varying refractive index. The predominant effect on a "small" antenna is that the varying refractive index introduces a pointing error. This has been recognized for some time in the case of satellite or missile tracking where a ground antenna is looking up at an angle through the atmosphere. In satellite tracking the steering data for the ground antennas is often corrected for elevation pointing errors by using a linearized model of the atmosphere (the index of refraction is assumed to vary exponentially with height) in calculating the needed correction.[17] There has also been interest in ray tracing methods, based upon meteorological data, to correct radar data for atmospheric refraction. This has been most successful in elevation angle

corrections,[5,10] but the method is also applied to azimuth corrections.[4]

Both the velocity and direction of radiation emanating from a point source will be affected as it traverses a region with a spatially varying refractive index. This would affect the time of arrival, and hence the phase of the radiation wavefront, at range R from the source. The effect on a receiving antenna system placed at range R is to introduce additional phase variations of the incoming signal across the antenna system. If the antenna is "small", the phase variation across the antenna is essentially linear and the effect is predominantly one of introducing a pointing error. The phase variation causes a warping of the phase front presented to a "large" antenna, however. For a long receiving antenna array the effect is similar to that of introducing phase errors along the array.

In the case of the synthetic aperture system there are also other sources of phase errors: radar platform motion, instability in the r. f. source and processor effects. The platform motion can be sensed and corrected for to within the limits of the sensors. Rapid progress is also being made in improving the stability of r. f. sources and in the area of data processors. However, little attention has been given to correcting the effects of propagation through the troposphere.

In this study an appropriate mathematical model of the synthetic aperture system is first developed, then extended to include the effects of propagation through a non-homogeneous medium (in this case the troposphere). An attempt is made here to develop a model of the atmospheric effects which best "fits" the experimental data available. A processing technique is then developed in which the processor calculates the

parameters of a phase filter matched in phase to the atmospheric turbulence being encountered.

II. THE SYNTHETIC APERTURE SYSTEM

1. MODEL AND PRELIMINARY ANALYSIS

It is instructive at this point to develop a mathematical model of the synthetic aperture system. Basically it consists of a coherent, side-looking radar which is moved in a straight line path at velocity, v. Typically it will be a pulse modulated radar. The relative phase and amplitude of the returned signal from each pulse transmission is stored for later data processing and, since the radar will move some distance, δx, between pulse transmissions, the single radar successively occupies the element positions in an array. As we shall see, there are advantages to be gained with the synthetic system, but there are also additional design restrictions.

Consider the flight path and target geometry of Figure 1, and let the transmitted signal be

$$f(t) = \mathrm{Re}\left\{A(t)\exp(i\omega_o t)\right\} \tag{1}$$

where $A(t)$ = envelope, typically pulse modulation and is a real time function,

ω_o = carrier frequency in radians per second

t = time, and i is $\sqrt{-1}$.

It will be convenient to let t be zero when x is zero. In order to obtain the complete beam pattern, we shall allow the x coordinate system to move relative to the target. The signal received at the n^{th} point, $n\delta x$ along the array, due to a point target at range R and $x = 0$, may be written

$$b(n\delta x,t) = \mathrm{Re}\left\{kA(t-\alpha)\exp\left[i\omega_o(t-\alpha)\right]F(n\delta x)\right\} \tag{2}$$

where k = constant related to range, reflectivity of target, etc.,

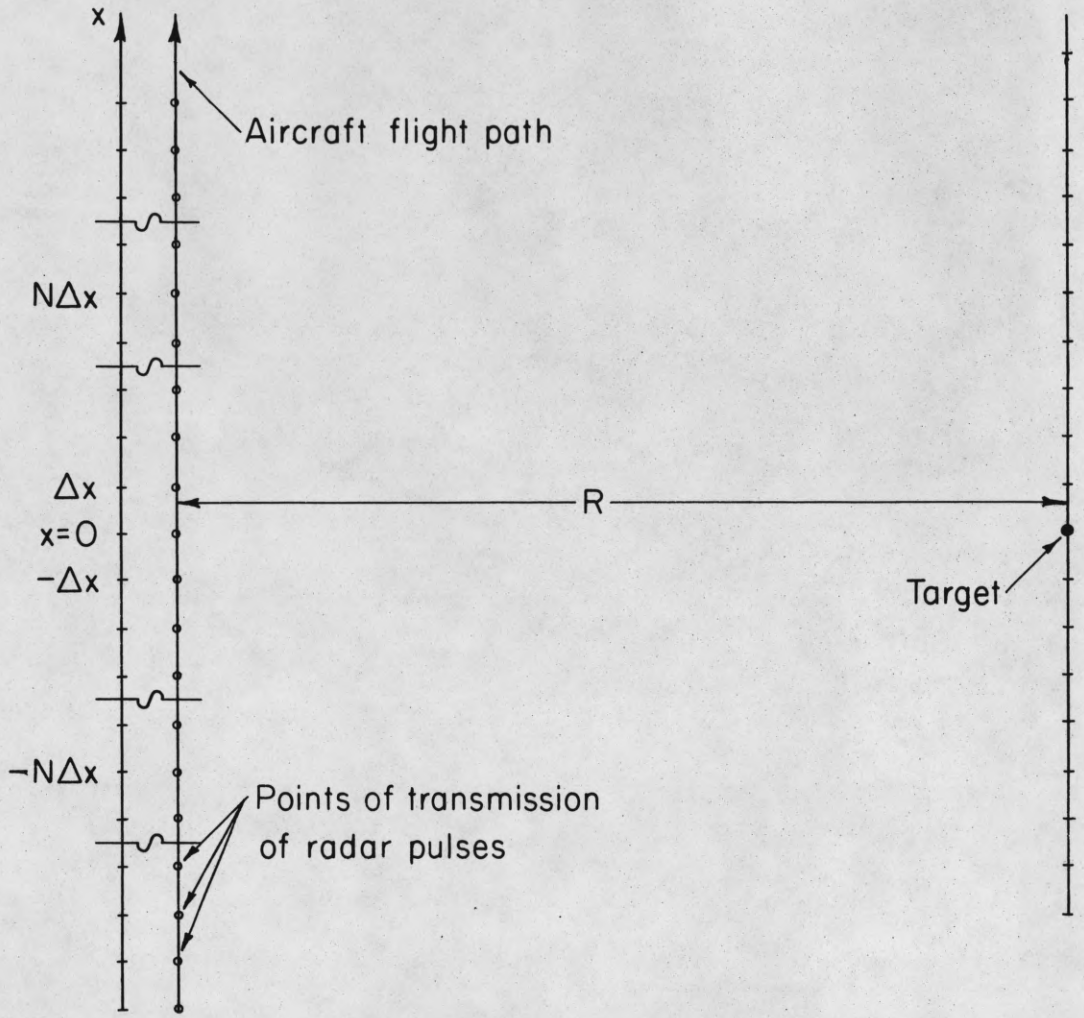

Figure 1. Basic Geometry

α = round-trip time delay to the target from the array position, $n\delta x$,

$F(n\delta x)$ = the synthetic array phase and amplitude weighting function used by the processor.

We may derive the expression for α as follows:

$$\alpha = \frac{2}{c}\left[\sqrt{R^2 + (n\delta x)^2}\right]$$

$$= \frac{2R}{c}\sqrt{1 + \frac{(n\delta x)^2}{R^2}}$$

$$= \frac{2R}{c}\left[1 + \frac{(n\delta x)^2}{2R^2} + \ldots\right]$$

$$\simeq \frac{2}{c}\left[R + \frac{(n\delta x)^2}{2R}\right], \qquad (3)$$

if $n\delta x \ll R$, which is the case here, and c is the velocity of propagation. Substituting (3) into (2) yields

$$b(n\delta x,t) = \mathrm{Re}\left\{kA\left(t - \frac{2}{c}\left[R + \frac{(n\delta x)^2}{2R}\right]\right)\exp(i\omega_o t)\exp\left(\frac{-i2\omega_o R}{c}\right)\right.$$

$$\left. F(n\delta x)\exp\left(-i\frac{\omega_o}{Rc}(n\delta x)^2\right)\right\}. \qquad (4)$$

The array output, $E(s,t)$, for this target is just the summation of the array returns or

$$E(s,t) = \sum_{n=s-N}^{s+N} b(n\delta x,t) \qquad (5)$$

for the array in position s (s is the parameter which allows the array to move relative to the target). If we let

$$A_R = A\left(t - \frac{2R}{c} - \frac{(n\delta x)^2}{Rc}\right) \simeq A\left(t - \frac{2R}{c}\right)$$

since $(n\delta x)^2 \ll 2R^2$, then (5) can be written

$$E(s,t) = \mathrm{Re}\left\{kA_R \exp\left[i\omega_o\left(t - \frac{2R}{c}\right)\right] \sum_{n=s-N}^{s+N} F(n\delta x)\exp\left(\frac{-i\omega_o (n\delta x)^2}{Rc}\right)\right\} \qquad (6)$$

2. PHASOR FORMULATION

Equation (4) can be represented in phasor form as

$$r(n\delta x, s) = kA_R F(n\delta x)\exp\left(\frac{-i\omega_o (n\delta x)^2}{Rc}\right) \qquad (4a)$$

if it is understood that the phasor is rotating at ω_o radians per second and that $-2\omega_o R/c$ is the reference phase of the phasor. The array output for range R and target at x = 0 can be written as the vector sum

$$R(s) = kA_R \sum_{n=s-N}^{s+N} F(n\delta x)\exp\left(\frac{-i\omega_o (n\delta x)^2}{Rc}\right). \qquad (7)$$

Choosing successive values for s, equivalent to allowing the array of 2N + 1 elements to move relative to the target, evaluates R(s) at the points s. The magnitude of R(s) at the points, s, yields points on the antenna beam pattern.

One of the advantages of the synthetic aperture system is that the processor can focus the array at all ranges concurrently. It can also steer the beam within limits. This is accomplished by a proper choice of $F(n\delta x)$. $F(n\delta x)$ can be written

$$F(n\delta x) = W(n\delta x)\exp\left[i\phi(n\delta x)\right],$$

where $W(n\delta x)$ represents the amplitude weighting function and $\phi(n\delta x)$ the phase weighting function. Amplitude weighting is commonly used to reduce side lobe levels and phase weighting to focus (or possibly steer) the array. For the time being let $W(n\delta x)$ equal one (uniform amplitude

weighting) and $\phi(n\delta x)$ focus the array at $s\delta x$ translated to range R,

$$W(n\delta x) = 1$$

$$\phi(n\delta x) = \frac{\omega_o}{Rc}(n\delta x - s\delta x)^2.$$

Equation (7) then becomes

$$R(s) = kA_R \sum_{n=s-N}^{s+N} \exp \frac{i\omega_o}{Rc}\left[(n\delta x - s\delta x)^2 - (n\delta x)^2\right]$$

$$= kA_R \exp\left(\frac{i\omega_o (s\delta x)^2}{Rc}\right) \sum_n \exp\left(\frac{-i2\omega_o n(\delta x)^2 s}{Rc}\right)$$

$$= kA_R \exp\left(\frac{-i\omega_o (s\delta x)^2}{Rc}\right) \frac{\sin\left[\frac{(2N+1)\omega_o (\delta x)s}{Rc}\right]}{\sin\left[\frac{\omega_o (\delta x)^2 s}{Rc}\right]}. \qquad (8)$$

The region of interest in equation (8) is usually only the main lobe and first few side lobes. If N is large then the small angle approximation to the sine can be made in the denominator and equation (8) becomes

$$R(s) = kA_R (2N+1) \exp\left(\frac{-i\omega_o (s\delta x)^2}{Rc}\right) \frac{\sin\left[\frac{(2N+1)\omega_o (\delta x)^2 s}{Rc}\right]}{\frac{(2N+1)\omega_o (\delta x)^2 s}{Rc}}. \qquad (9)$$

The magnitude of equation (9) yields the familiar pattern associated with equally weighted synthetic arrays. It has a maximum of $(2N+1)kA_R$ at $s = 0$ and zeros (nulls) at

$$s = \frac{Rc\ell\pi}{(2N+1)\omega_o (\delta x)^2}, \qquad \ell = \pm 1, 2....$$

(The derivation thus far parallels quite closely that of H. L. McCord.[13] It differs from his in that the antenna is moved to obtain the pattern,

rather than the target.)

Amplitude weighting can be used to reduce the level of the side lobes, but at the expense of widening the main lobe.

Equation (9) can be made dimensionless by specifying the distances in terms of the radiation wavelength. We can write

$$\frac{\omega_o}{Rc} = \frac{2\pi f}{Rc} = \frac{2\pi\lambda}{R} = \frac{2\pi}{R}$$

where R is now to be given in wavelengths. Then (9) becomes

$$R(s) = kA_R(2N+1)\exp\left(\frac{-i2\pi(s\delta x)^2}{R}\right)\frac{\sin\left[\frac{2\pi(2N+1)(\delta x)^2 s}{R}\right]}{\frac{2\pi(2N+1)(\delta x)^2 s}{R}}, \qquad (10)$$

where all dimensions are in wavelengths.

3. MAXIMUM RESOLUTION CAPABILITY AND SOME DESIGN RESTRICTIONS

In order to obtain useful information about a particular target from each of 2N + 1 recorded received signals, the target must be within the beamwidth of the antenna used with the coherent radar for each of the 2N + 1 element positions the antenna assumes in forming the synthetic array. Therefore, the maximum useful length that a synthetic array can have is a function of the range, R, and the beamwidth of the antenna used with the coherent radar. The width of the radiated beam, in radians, is given by the ratio λ/D, where D is the horizontal aperture size of the antenna used. If D is measured in wavelengths, this becomes 1/D. The maximum useful length for the synthetic array, $\left[(2N+1)\delta x\right]_{max}$, is the width of the physical antenna beam at the range R,

$$\left[(2N+1)\delta x\right]_{max} = \frac{R}{D}.$$

If this maximum length is used in equation (10), then

$$R(s) = kA_R(2N+1)\exp\left(\frac{-i2\pi(s\delta x)^2}{R}\right)\frac{\sin\left(\frac{2\pi s\delta x}{D}\right)}{\frac{2\pi s\delta x}{D}} . \qquad (11)$$

It is interesting to note that the first zeros of this equation (often taken as a measure of beamwidth) occur at

$$s\delta x = \pm\frac{D}{2}.$$

Note that the ultimate beamwidth (and hence the azimuth resolution) is independent of range and wavelength.[6,8] The implication is that finer resolution is achievable by using a small antenna, rather than a large one, with the coherent radar. This is not the only criterion to be used in the selection of the antenna size, however. In the real case there will be targets throughout the region radiated by the antenna beam. Since the radar platform is moving at velocity, v, there will be a doppler shift in the returned signal (a frequency spread in the case of multiple targets). Because of the finite width of the physical antenna beam, there will be a maximum doppler shift, $(fd)_{max}$. With a pulse radar this frequency spread is sampled at the pulse recurrence frequency (PRF). According to the sampling theorem, the minimum sampling rate must be twice the maximum frequency component, $(fd)_{max}$. If the physical antenna is pointed perpendicular to v, $(fd)_{max}$ is given by

$$(fd)_{max} = \frac{2v}{\lambda}\sin\left(\frac{\lambda}{2D}\right)$$

$$\simeq \frac{v}{D},$$

if $\lambda \ll D$. Correspondingly the minimum pulse recurrence frequency, PRF,

(according to the sampling theorem) must be

$$(PRF)_{min} = 2(fd)_{max}$$
$$\simeq \frac{2v}{D}.$$

However, the PRF is determined by the maximum range to be processed, and v must be compatible with the possible speed of the aircraft carrying the radar platform. Thus there are other factors influencing the choice of the antenna size.

For more information concerning the synthetic aperture radar system, including sample radar pictures, see references 1, 6, 8, 11, 13 and 16.

III. THE ATMOSPHERIC TURBULENCE PROBLEM

The development of the previous chapter assumed an ideal system (the radar and processor), operating in an ideal, homogeneous propagation medium. In this chapter we shall assume an ideal system and develop a mathematical model to show the effects of a non-homogeneous propagation medium (the troposphere).

1. THE EFFECT OF ATMOSPHERIC TURBULENCE

The troposphere is in a continuous turbulent motion. There are both horizontal and vertical fluctuations of temperature, pressure, and humidity which cause a departure from homogeneity and result in a spatially varying refractive index. The spatial autocorrelation function for the refractive index is normally assumed to be a function only of the distance between the two points at which the index is measured and not of their location in space. The width, ℓ_o, of the autocorrelation function for the refractive index is a measure of the scale of the atmospheric turbulence. As such it would be expected to depend to some degree on position and time. Some form of exponential correlation function is most commonly assumed.[1,12,14]

If we consider a point source of radiation, we would expect a ray emanating from it to undergo a series of random phase delays as it encounters first more dense then less dense regions of the troposphere. Bending would also occur as it traversed a path to a receiving antenna. The lengthening of the path caused by bending, however, has only a second order effect on the phase reaching the receiving antenna. If an appropriate correlation function for the refractive index is assumed, then an approximate correlation function for the phase at a distance R from the

source can be derived.[14] It is sufficient for our purpose here, however, to assume that the autocorrelation function for the phase is a function of the distance R and of the spacing of the two points at which the phase is measured. The width of the phase autocorrelation function we shall refer to simply as the "correlation length". It is likely that some form of exponential correlation function would be appropriate for the phase also.

If the dimensions of the antenna are small compared to the correlation length, then the signal from the point source arrives at the antenna as essentially a plane wave, but the apparent direction of arrival may differ slightly from the straight line path between source and antenna. The atmosphere has introduced a phase error with essentially constant gradient across the antenna, effectively causing a pointing error. This pointing error would be a function of space and time. Moving the antenna to a new location where it was "looking" through a different volume of space should lead to a different pointing error. On the other hand, the atmosphere does change with time, although relatively slowly. If the antenna is left fixed, the time change of the atmosphere would lead to a changing pointing error.

The pointing error associated with a "small" antenna is not of primary interest to the problem being developed here, since resolution is not affected. We can, however, gain some insight about the "turbulent atmosphere" by pursuing it further.

A pointing error equivalent to that caused by the atmosphere could be effected by introducing a linear phase change across the antenna. It seems reasonable to assume that we can consider the "lumped equivalent"

of the atmosphere as a phase error across the antenna.

If a "small" antenna is used to observe the signal from a point source placed some distance away, the apparent direction from which the signal is coming will change slowly with time. Over a long period of time one would expect the atmospheric effect at the "small" antenna to go through similar variations to what would be expected if the antenna were moved through the atmosphere at constant range from the point source. Over a long period of time, assuming that each observation of pointing error took place in a time short with respect to the time of variation of the atmosphere, the statistics of a large number of observations would give statistics concerning the effective slope of the wavefront reaching the antenna. Such experimental readings were made at White Sands Missile Range in New Mexico.[4] The azimuth pointing error readings are of importance here. The statistics of a large number of azimuth readings showed no significant departure from a Gaussian distribution. The mean observed value corresponded almost exactly to the geometric azimuth angle, with a standard deviation of about 0.12 milliradians and peak observed deviation of approximately $\pm$ 0.50 milliradians. The distance between point source and antenna was about 45 miles.

If we now consider an antenna which is long compared to the phase correlation length associated with the atmosphere we might observe a "phase front" similar to that shown in Figure 2, where Figure 2 shows a representative member function of the set of possible phase fronts. The effect of such a phase front on a small antenna would be one of steering and the possible pointing errors versus position on the curve would be a reasonable fit to the statistics above. For a "small" antenna the curve

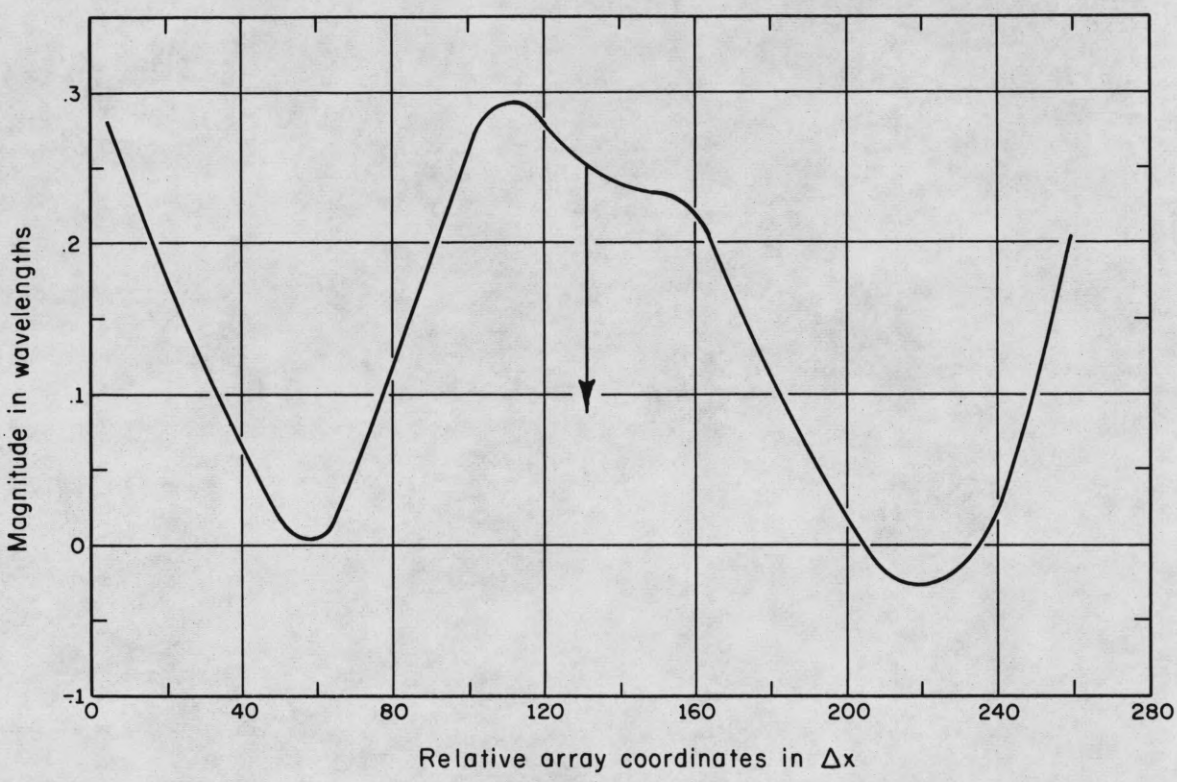

Figure 2. Member Function of the Set of Possible Radiation Phase Fronts

of Figure 2 represents pointing errors ranging from +0.5 to -0.35 milliradians. Actually observations indicate that there would be a somewhat higher frequency variation superimposed on such a phase front, but that its amplitude would be small. We shall neglect this in this development. We would also expect that the amplitude of the phase front (amount of phase error) is a function of the range to the source. Subject to reasonable assumptions it has been shown to be directly proportional to range.[1] The results of other experiments,[9,12] are in substantial agreement with the above results.

For an antenna that is long compared to the correlation length, the phase front reaching the antenna, under the above assumptions, would be distorted in some fashion similar to Figure 2. The non-homogeneous atmosphere is seen at the antenna as a "phase noise". We are assuming then that the atmospheric turbulence effect can be considered as a multiplicative noise at the antenna, a noise which is a function of the dimension along the antenna.

2. MATHEMATICAL FORMULATION FOR A SINGLE TARGET

As pointed out in the previous chapter, synthetic arrays designed to give very high resolution could be quite long, and they are likely to be long compared to the phase correlation length of the atmosphere. To obtain the synthetic array beam pattern, the array of $2N + 1$ elements is moved perpendicular to a line representing the range to a single target (see Figure 1). In this way it is possible to represent the real case when phase noise due to the atmosphere is present. The target and the equivalent phase noise at the plane of the antenna stay

fixed in space and the antenna of 2N + 1 elements moves relative to the noise and target. This is in contrast to a more conventional approach to including atmospheric phase noise in the synthetic system,[11] but was deemed necessary to obtain a true picture of the effect of atmospheric turbulence. The development of Chapter 1 is compatible with this approach and will now be extended to include phase noise.

Equation (7), rewritten such that all units of length are in wavelengths and hence dimensionless, becomes

$$R(s) = kA_R \exp\left(\frac{i2\pi(s\delta x)^2}{R}\right) \sum_{n=s-N}^{s+N} \exp\left(\frac{-i4\pi n(\delta x)^2 s}{R}\right), \qquad (12)$$

where the target is at x = 0, the array is uniformly weighted and focused at range R and x = sδx.

In our model atmospheric turbulence causes a multiplicative noise term which is a function of x and is of unit amplitude (this exludes any multi-path transmission):

$$PN(n\delta x) = \exp\left[-i\Theta(n\delta x)\right].$$

Including this, R(s) becomes

$$R(s) = kA_R \exp\left(\frac{i2\pi(s\delta x)^2}{R}\right) \sum_{n=s-N}^{s+N} \exp\left\{-i\left[\frac{4\pi n(\delta x)^2 s}{R} + \Theta(n\delta x)\right]\right\}. \qquad (13)$$

In order to include the main lobe and the first few side lobes, the range of s would be $-B/2 \leq s \leq B/2$, with B even.

The multiplicative noise and array lengths being considered are such that $\Theta(n\delta x)$ only goes through a small number of "cycles" in the distance (2N+B)δx, implying that the first few terms of a Fourier series should provide an approximation to the noise with little error. We can

write the approximation as

$$\Theta(n\delta x) = \sum_{m=1}^{K} a_m \cos\left[\frac{2\pi(mn + b_m)\delta x}{(2N+B)\delta x}\right]; \qquad (14)$$

using this, equation (13) becomes

$$R(s) = kA_R \exp\left(\frac{i2\pi(s\delta x)^2}{R}\right) \sum_n \exp\left\{-i\left[\frac{4\pi n(\delta x)^2 s}{R} + \sum_m a_m \cos\left(\frac{2\pi(mn + b_m)}{2N+B}\right)\right]\right\}. \qquad (15)$$

It is quite common to use amplitude weighting to reduce the magnitude of the pattern side lobes. Cosine squared weighting is perhaps the most common. Equation (15) can be written to include this as follows:

$$R(s) = kA_R \exp\left(\frac{i2\pi(s\delta x)^2}{R}\right) \sum_n \cos^2\left(\frac{\pi(n-s)}{2N}\right) \exp\left\{-i\left[\frac{4\pi n(\delta x)^2 s}{R} + \sum_m a_m \cos\left(\frac{2\pi(mn + b_m)}{2N+B}\right)\right]\right\} \qquad (16)$$

Note that the noise enters in as a phase modulation in equations (15) and (16). One would expect the effects of the noise phase-modulation to be similar to that of phase-modulation of a carrier frequency: namely, that low modulation amplitude gives rise to only an upper and a lower sideband of significant level and displaced from the carrier by an amount proportional to the modulation frequency. Increasing the level of modulation gives rise to an increasing number of sidebands of significant level, separated by an amount proportional to the modulation frequency. The energy for these sidebands must come from the carrier, so that as the sideband levels increase, the carrier level decreases. It is possible to put all of the carrier energy into the sidebands. Analogous to the carrier, we have the main lobe of the pattern, to the sidebands, undesired side lobes. The side lobes for "low frequency" modulation may fall within

the main lobe and tend to broaden it, while higher frequencies cause distinct side lobes. An additional effect to be noted, analogous to ramp modulation of a carrier, is a beam pointing error.

Equations (15) and (16) were solved for representative values of a_m and b_m for m ranging from one to six. Curves showing the results, with only one harmonic at a time are shown in Figures 3 through 14, illustrating that the behavior is analogous to the phase modulation. Figures 9 through 14 show the effect of such "noise" terms if cosine squared amplitude weighting is used. For each of these curves a_m for the harmonic used was set at pi radians, $b_m = 0$. The resulting pattern distortion is severe and would essentially destroy the usefulness of the array. Lower values of the a_m were also used, with similar, but less severe, distortion resulting. In comparing the effect on the uniform weighted with the effect on the cosine squared weighted, it will be noted that the pattern is perturbed less for the first harmonic with cosine squared weighting. For the higher harmonics, the distortion caused is quite similar. It should be noted that the symmetry exhibited by the curves of Figures 3 through 14 exists only if the period of the phase modulation is harmonically related to $(2N+B)\delta x$, the length associated with the number of elements used in processing.

The results with single harmonics, however, can only be used as a guide to the behavior when the harmonics are used in combination to approximate phase noise. Taking the magnitude of R(s) is a non-linear process and superposition does not hold. Figures 15 and 16 show an example of the perturbed beam patterns for uniform and cosine squared weighting, respectively, when the harmonics are used in combination to produce the phase front shown as Figure 17.

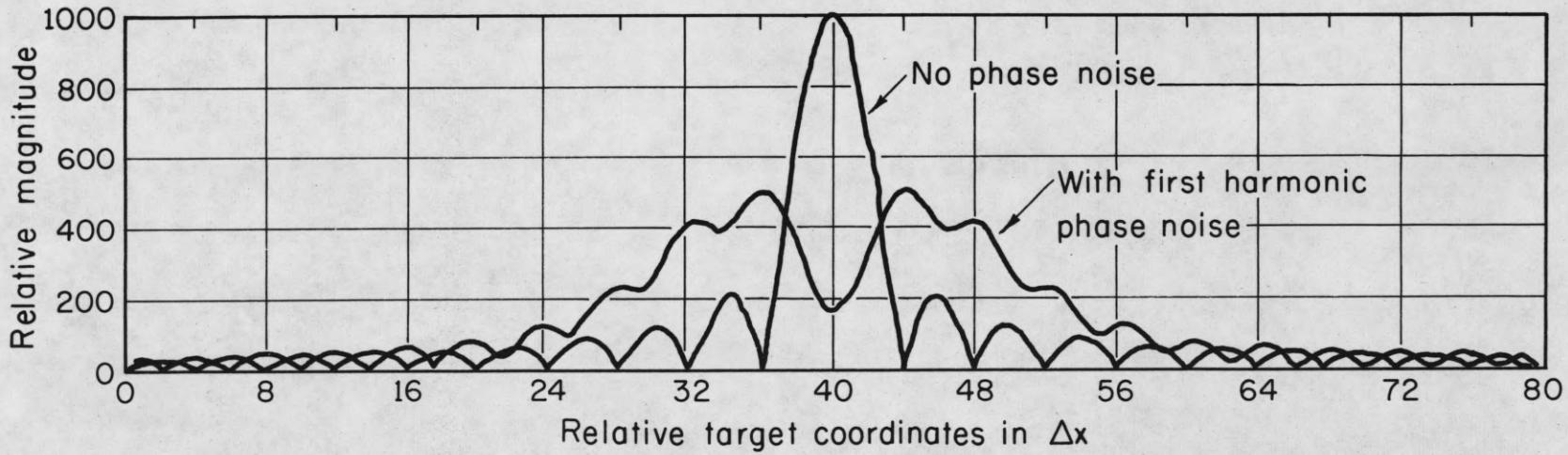

Figure 3. System Output Beam Pattern, Uniform Weighting, No Noise and First Harmonic Phase Noise at 1.0λ Peak to Peak

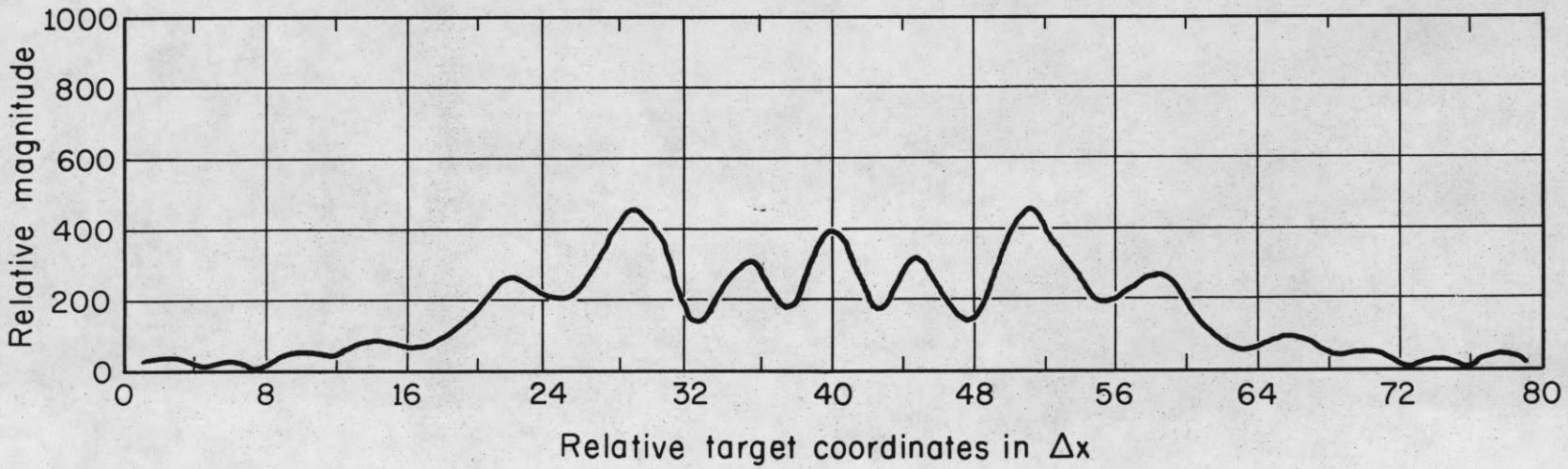

Figure 4. Beam Pattern, Uniform Weighting, Second Harmonic, 1.0λ Peak to Peak

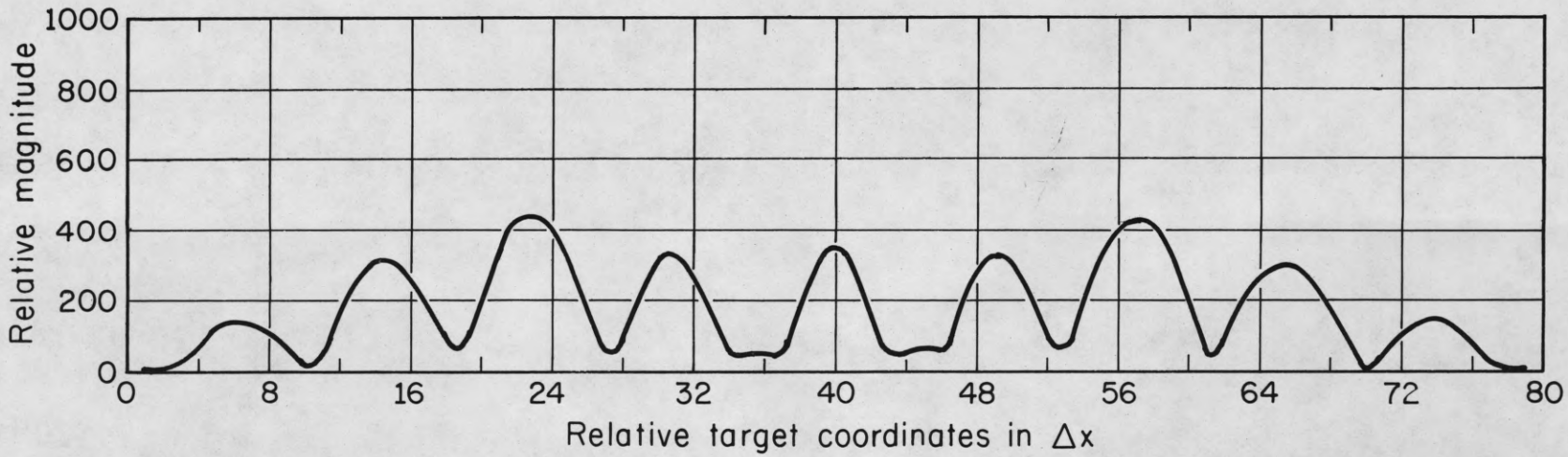

Figure 5. Beam Pattern, Uniform Weighting, Third Harmonic, 1.0λ Peak to Peak

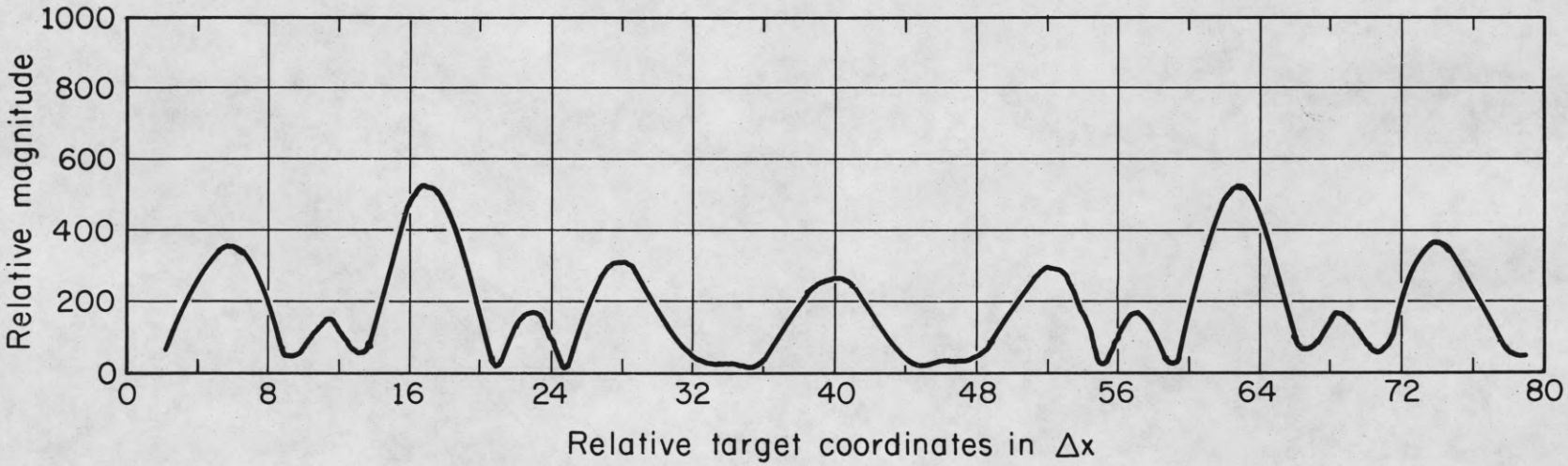

Figure 6. Beam Pattern, Uniform Weighting, Fourth Harmonic, 1.0λ Peak to Peak

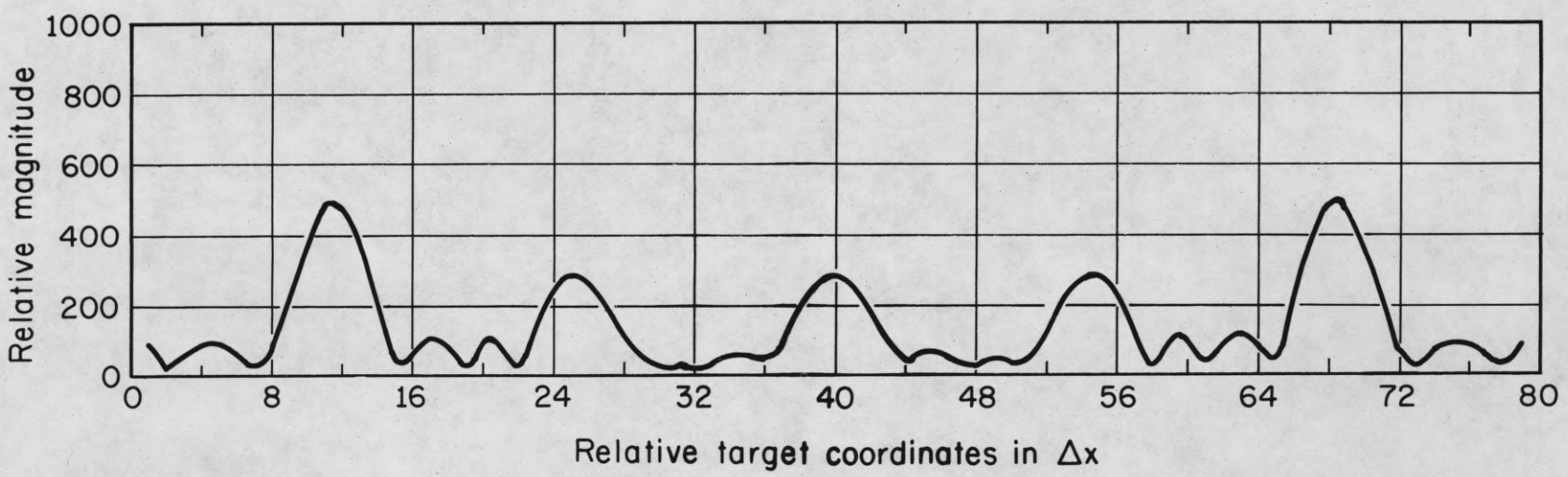

Figure 7. Beam Pattern, Uniform Weighting, Fifth Harmonic, 1.0λ Peak to Peak

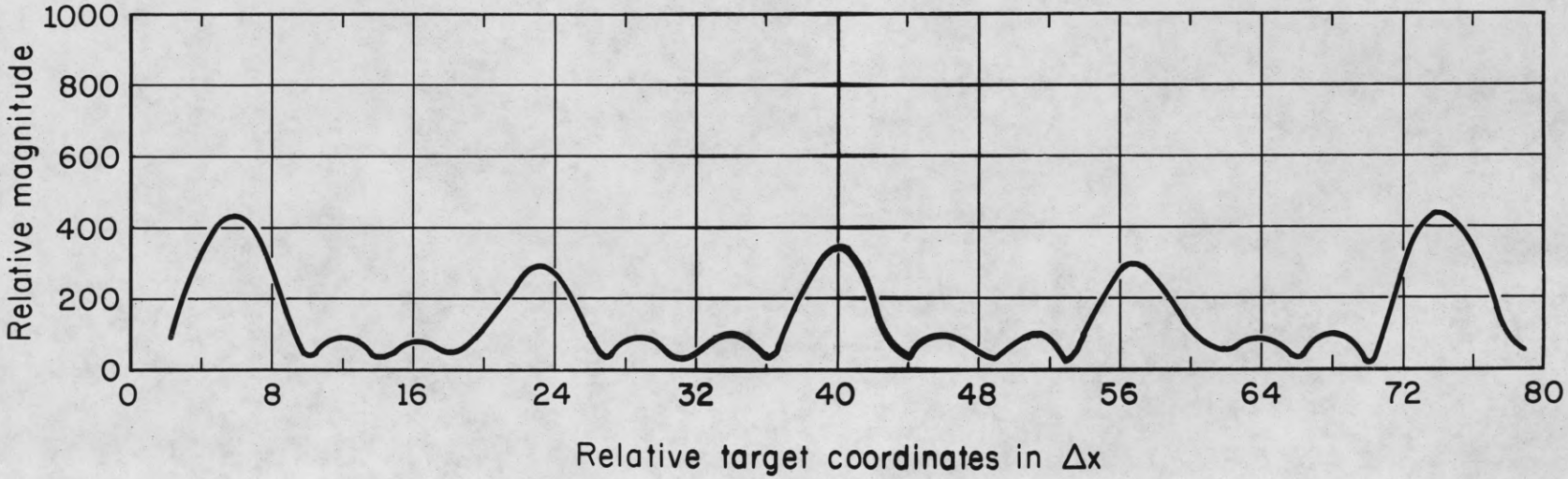

Figure 8. Beam Pattern, Uniform Weighting, Sixth Harmonic, 1.0λ Peak to Peak

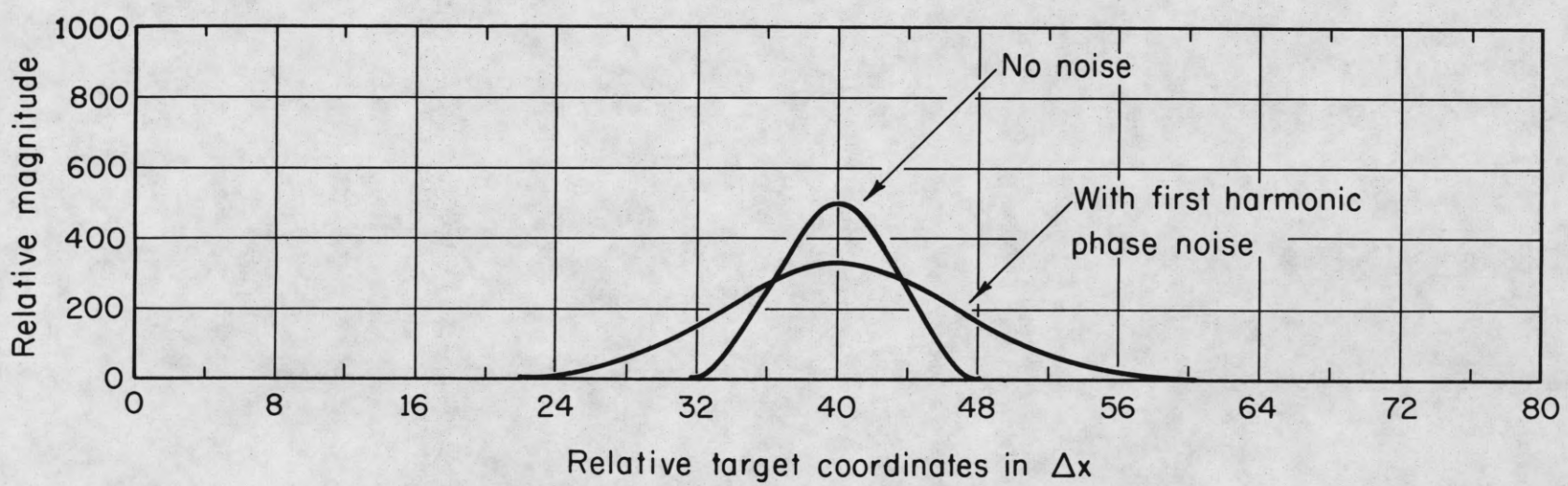

Figure 9. Beam Pattern, Cosine Squared Weighting, No Noise and First Harmonic at 1.0λ Peak to Peak

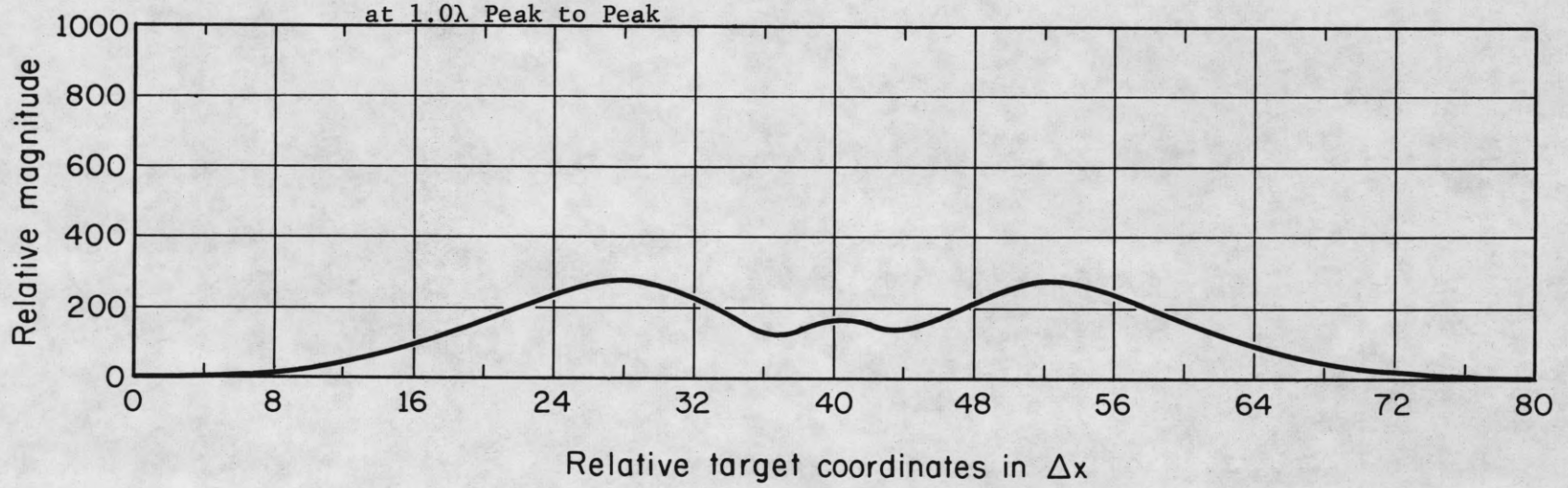

Figure 10. Beam Pattern, Cosine Squared Weighting, Second Harmonic, 1.0λ Peak to Peak

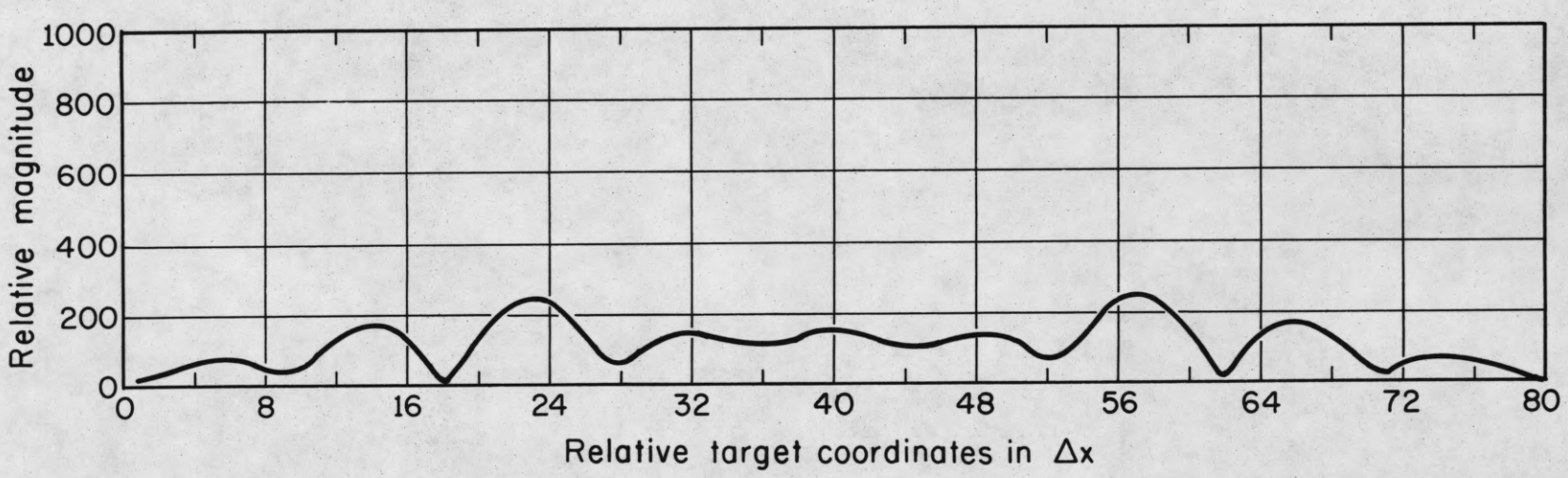

Figure 11. Beam Pattern, Cosine Squared Weighting, Third Harmonic, 1.0λ Peak to Peak

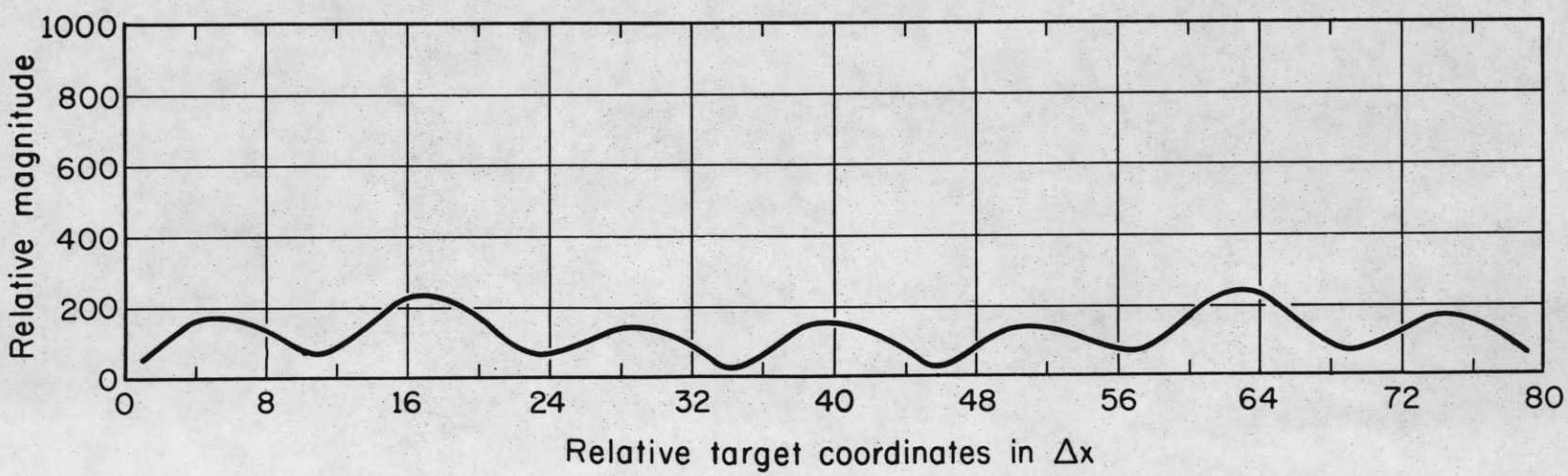

Figure 12. Beam Pattern, Cosine Squared Weighting, Fourth Harmonic, 1.0λ Peak to Peak

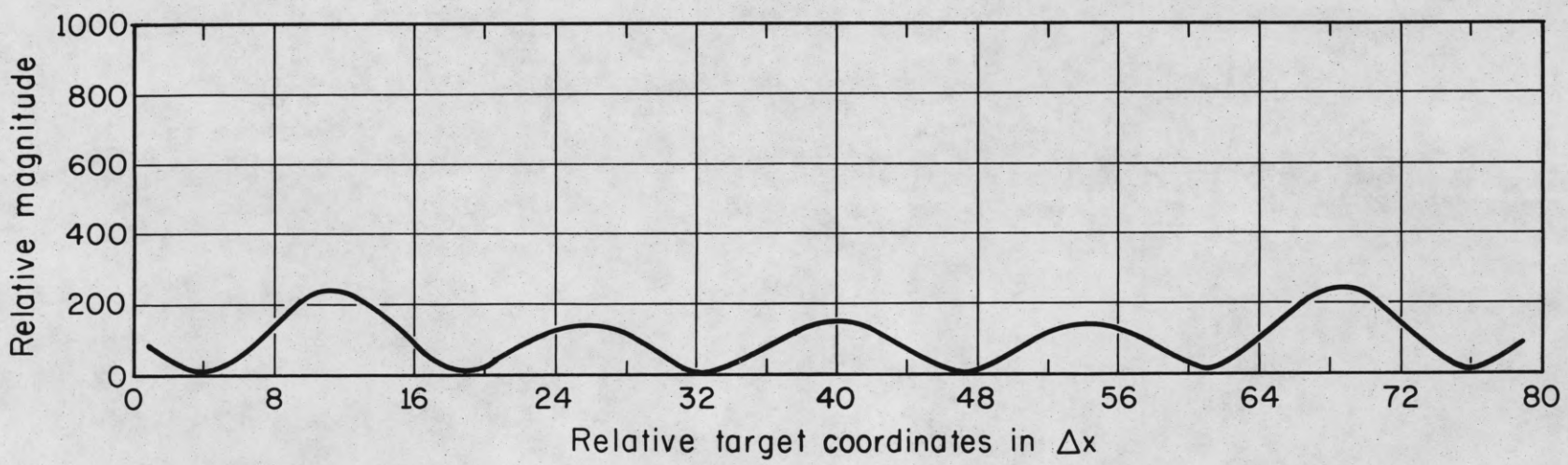

Figure 13. Beam Pattern, Cosine Squared Weighting, Fifth Harmonic, 1.0λ Peak to Peak

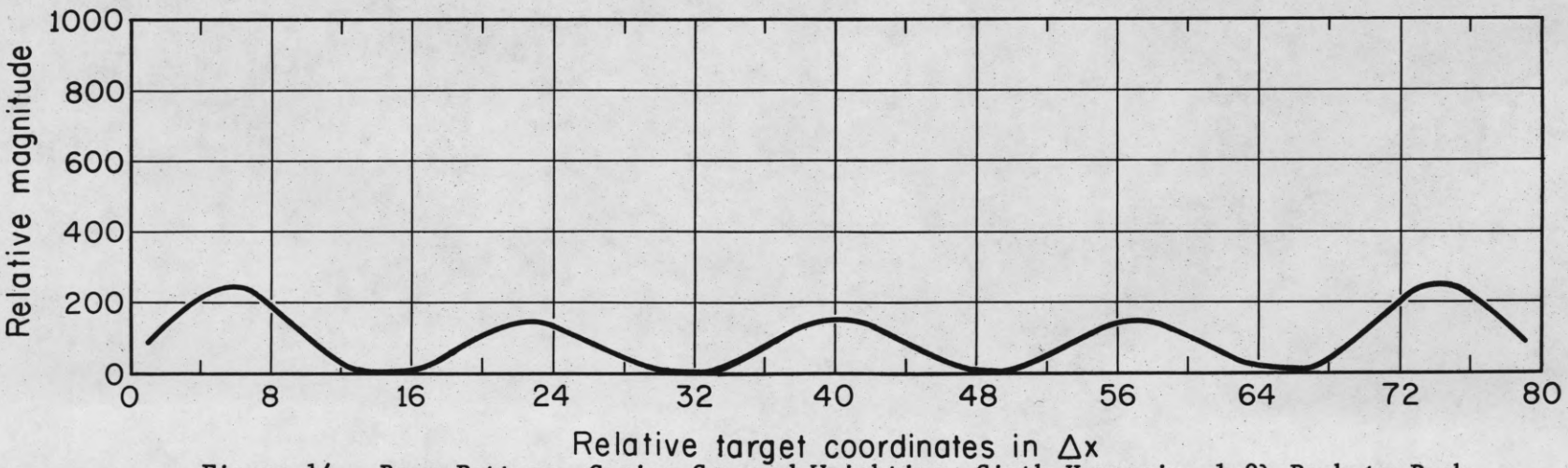

Figure 14. Beam Pattern, Cosine Squared Weighting, Sixth Harmonic, 1.0λ Peak to Peak

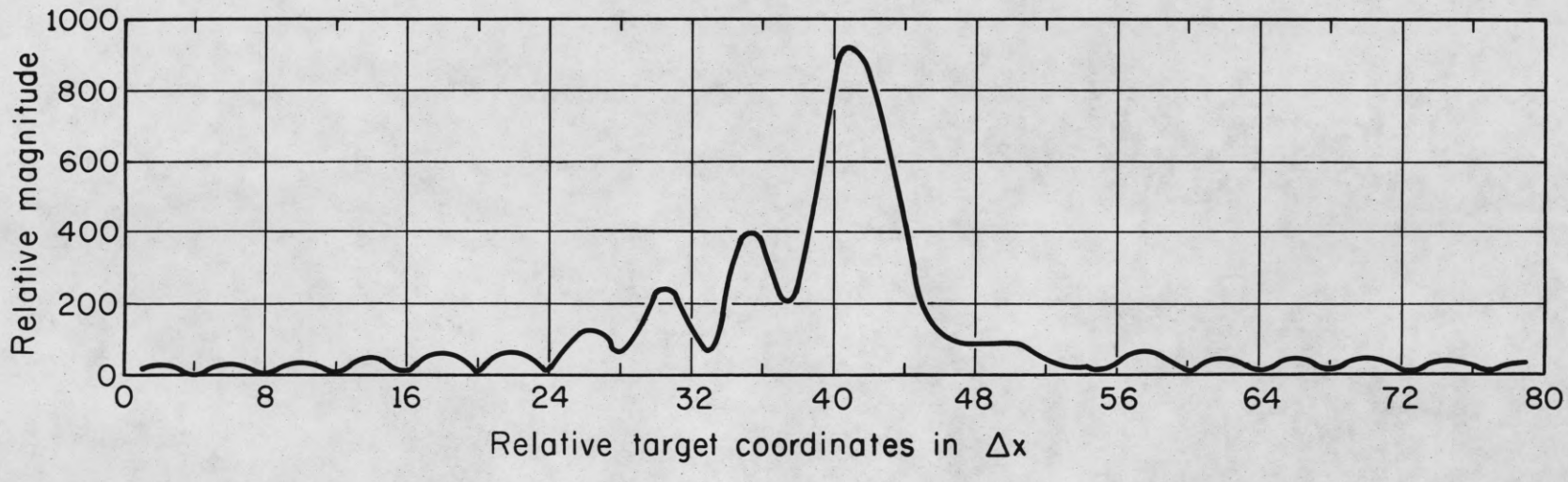

Figure 15. Beam Pattern, Uniform Weighting, Perturbed by Phase Front Shown in Figure 17

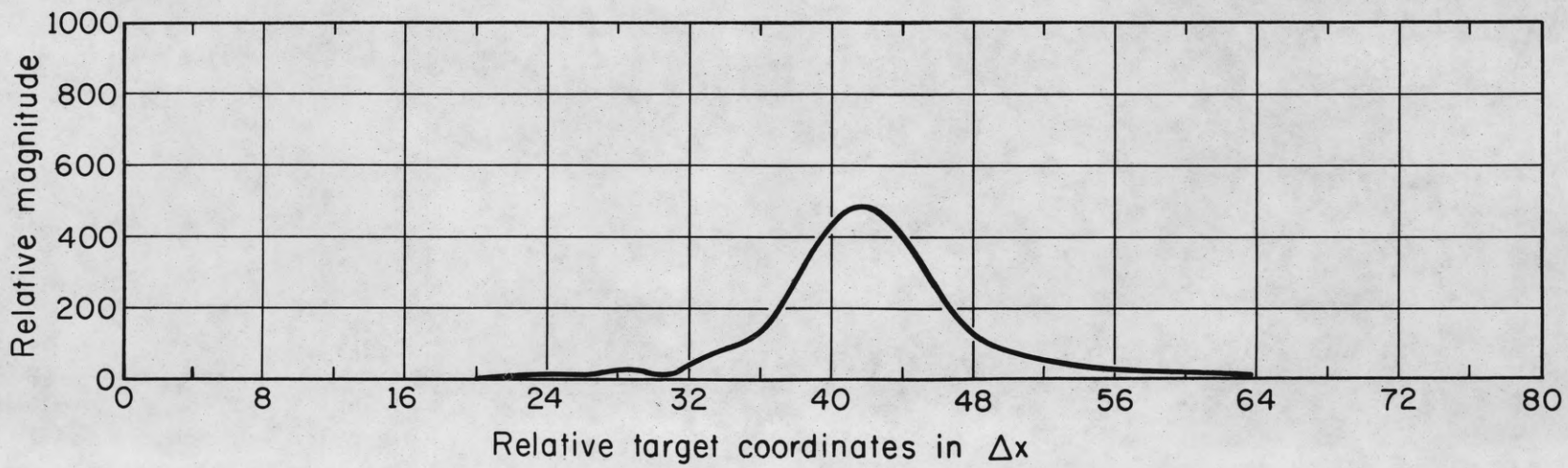

Figure 16. Beam Pattern, Cosine Squared Weighting, Perturbed by Phase Front Shown in Figure 17

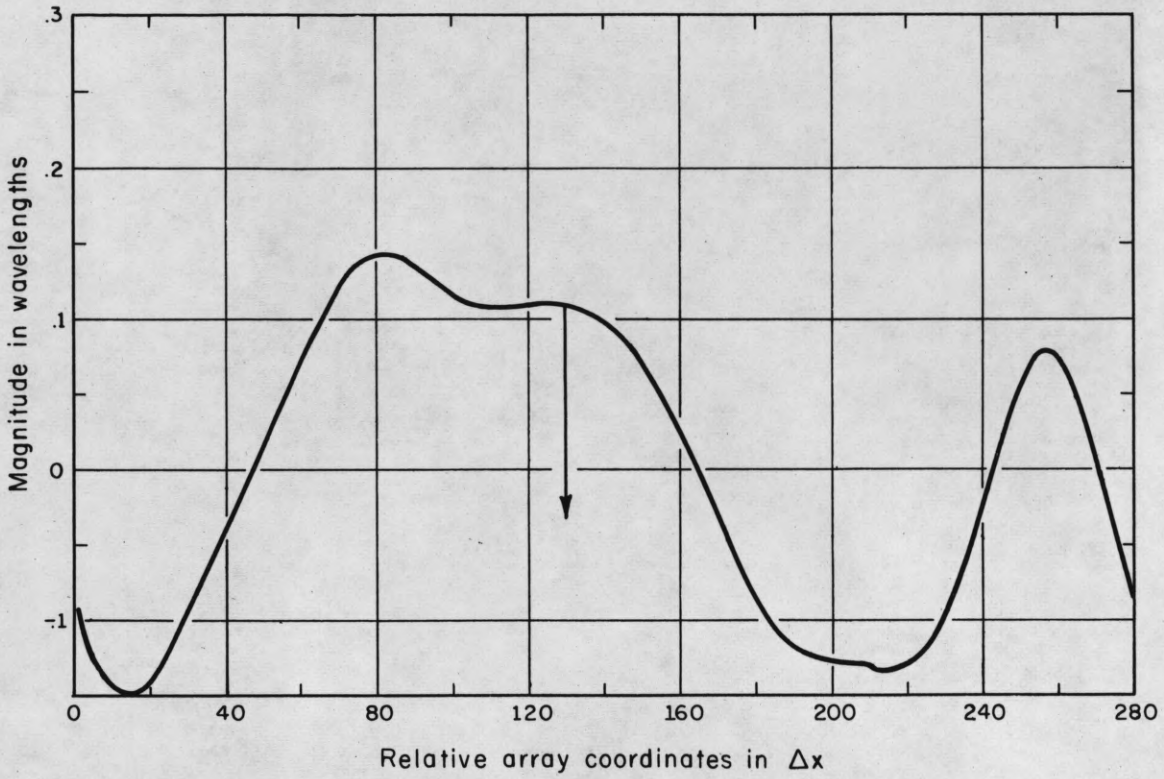

Figure 17. Simulated Radiation Phase Front, First Six Harmonics Used

3. MULTIPLE TARGET ANALYSIS

While it is interesting (and necessary) to consider the behavior of the beam pattern (single target) when the synthetic array is subjected to phase noise, we should extend our discussion to include the effects when multiple targets are within the individual element beam. We shall assume that the processor operates on each range independently (actually a small range interval, determined by the effective pulse width of the modulation used). As an approximation to actual target structure, we will use point targets (at the range to be processed) with random spacing, reflection amplitude and phase. For later convenience in the computer simulation let the allowed target locations correspond to the antenna element positions translated to the range, R. The signal received at the n^{th} point, $n\delta x$ along the array, will be the vector summation of the signals returned from all of the targets within the beamwidth of the coherent radar antenna when it is at position $n\delta x$, taking into account the differences in transmission path lengths. Following a development similar to that of Chapter 1, we can write the phasor equation, analogous to equation (4a) as

$$r(n\delta x, s) = F(n\delta x) \sum_{k=\left[n-\frac{R\phi}{2\delta x}\right]}^{\left[n+\frac{R\phi}{2\delta x}\right]} A(k)\exp\left[-i\, f(n,k)\right] \qquad (17)$$

where $F(n\delta x)$ is as defined for equation (2), ϕ is the beamwidth of the coherent radar used, in radians, $A(k)$ is a constant related to range to and reflectivity of the target at location k, and $f(n,k)$ is a function accounting for differences in path lengths and phase centers of the target.

A(k) will be zero unless k corresponds to a target location and $[x]$ is to be interpreted as the largest integral value of x.

$$f(n,k) = 2\pi\left[2\sqrt{R^2 + (n\delta x - k\delta x)^2} + P(k)\right]$$

$$= 2\pi\left[2R\sqrt{1 + \frac{(n\delta x - k\delta x)^2}{R^2}} + P(k)\right]$$

$$\cong 2\pi\left[2R + \frac{(n\delta x - k\delta x)^2}{R} + P(k)\right], \qquad (18)$$

if $(n\delta x - k\delta x) \ll R$, which is the case here.

Substituting (18) into (17) and simplifying yields

$$r(n\delta x,s) = F(n\delta x) \sum_{k=\left[n-\frac{R\phi}{2\delta x}\right]}^{\left[n+\frac{R\phi}{2\delta x}\right]} A(k)\exp\left\{-i2\pi\left[\frac{(n-k)^2(\delta x)^2}{R} + P(k)\right]\right\}. \qquad (19)$$

As before, the array output is the summation of the $r(n\delta x,s)$,

$$R(s) = \sum_{n=s-N}^{s+N} r(n\delta x,s),$$

where $r(n\delta x,s)$ is defined by (19).

For uniform weighting, $F(n\delta x)$ takes the form

$$F(n\delta x) = \exp\left(\frac{i2\pi(n-s)^2(\delta x)^2}{R}\right),$$

which focuses the array at $s\delta x$ translated to range R. Then

$$R(s) = \sum_{n=s-N}^{s+N} \exp\left(\frac{i2\pi(n-s)^2(\delta x)^2}{R}\right) \sum_{k=\left[n-\frac{R\phi}{2\delta x}\right]}^{\left[n+\frac{R\phi}{2\delta x}\right]} A(k)\exp\left\{-i2\pi\left[\frac{(n-k)^2(\delta x)^2}{R} + P(k)\right]\right\} \qquad (20)$$

Since this is already in a form that is convenient for computer use,

there is no point in altering its form. For cosine squared weighting, R(s) becomes

$$R(s) = \sum_n \cos^2\left(\frac{\pi(n-s)}{2N}\right) \exp\left(\frac{i2\pi(n-s)^2(\delta x)^2}{R}\right) \sum_k A(k) \exp\left\{-i2\pi\left[\frac{(n-k)^2(\delta x)^2}{R} + P(k)\right]\right\} \qquad (21)$$

Actually equations (20) and (21) illustrate the division between summations performed by the processor and summing performed naturally at the coherent radar antenna. The second summation in each equation occurs at the radar antenna; while the first summation must be performed by the processor.

We would like to be able to add the atmospheric noise terms in as was done in equations (15) and (16). However, some thought must be given as to what the noise terms should look like in the case of multiple targets. In the case of multiple targets, each target would have a different multiplicative noise term at the array due to atmospheric turbulence, since the path between each and a given array element position is different. However, the paths for adjacent targets do not differ significantly and one would expect them to have nearly identical noise terms. In fact, since we can also define a phase autocorrelation function (and a correlation length) for the atmospheric turbulence effects at the targets at range R, we would expect nearly identical noise terms for a group of targets which are well within the correlation length. If the range of $s\delta x$ for one processing interval, $-B\delta x/2 \leq s\delta x \leq B\delta x/2$, is set to well within the correlation length, then a single noise term gives a good approximation to the effect of the atmosphere on targets within the

interval. This noise term would become progressively worse as an approximation for targets outside the interval as the distance from the interval increases. For relatively low noise level it seems reasonable to assume that targets far enough outside the interval to be affected by significantly different noise terms have little effect on the targets within the interval. The undesired side lobes from such targets become insignificant in magnitude in the interval being processed. This is equivalent to assuming that only one noise term need be associated with all of the targets influencing the processing within the interval.

Including the noise term, R(s) becomes

$$R(s) = \sum_{n=s-N}^{s+N} \exp\left\{ i\left[\frac{2\pi (n-s)^2 (\delta x)^2}{R} + \sum_{m=1}^{K} a_m \cos\left(\frac{2\pi (mn+b_m)}{2N+B} \right) \right] \right\} \sum_{k=\left[n - \frac{R\Phi}{2\delta x}\right]}^{\left[n + \frac{R\Phi}{2\delta x}\right]} A(k) \exp$$

$$\left\{ -i2\pi \left[\frac{(n-k)^2 (\delta x)^2}{R} + P(k) \right] \right\}, \qquad (22)$$

for uniform weighting and

$$R(s) = \sum_{n} \cos^2\left(\frac{\pi (n-s)}{2N} \right) \exp\left\{ i\left[\frac{2\pi (n-s)^2 (\delta x)^2}{R} + \sum_{m} a_m \cos\left(\frac{2\pi (mn+b_m)}{2N+B} \right) \right] \right\}$$

$$\sum_{k} A(k) \exp\left\{ -i2\pi \left[\frac{(n-k)^2 (\delta x)^2}{R} + P(k) \right] \right\} \qquad (23)$$

for cosine squared weighting.

IV. A SOLUTION TO THE ATMOSPHERIC TURBULENCE PROBLEM

1. RESTATING THE PROBLEM

The development of the last chapter concentrated on what the effects of the atmosphere are. If one considers possible means of removing the effects, the problem takes on a somewhat different character.

The object of any processor would be to gain optimum information about the A(k) of equations (22) and (23). The data (recorded received signals) it has to work with are corrupted by multiplicative noise due to the atmosphere. Subject to the assumptions made, we know the general character of the multiplicative noise; although we must recognize that the Fourier representation used is only an approximation to the actual noise (for finite K).

After considering the possibilities, one is led quite naturally to the conclusion that what is needed is an adaptive matched filter: a filter that is matched to the atmospheric phase noise affecting the interval being processed. Adaptive in that it must "learn" by some means just what the phase noise is in order to achieve the matched condition. All that is available to "learn" from are the recorded received signals from the range (or ranges) being processed.

2. THE PROCESSOR

Various means of obtaining the desired information about the phase noise by averaging techniques were considered and then discarded as unworkable. One method that was successful for the model used is to consider the problem as a "simple" control problem. Let the matched filter phase be the control variable and adjust it according to some

criterion — some definable function that can be either maximized or minimized as the case may be.

The recorded received signals from range R could be written as

$$s(n\delta x) = A(n)\exp\left[i\Theta(n)\right],$$

where $\Theta(n) = \Theta(n)_{signal} + \Theta(n)_{noise}$, in radians. The system output for a focused, uniform weighted array would be

$$R(s) = \sum_{n=s-N}^{s+N} A(n)\exp\left\{i\left[\frac{2\pi(n-s)^2(\delta x)^2}{R} + \Theta(n)\right]\right\}. \qquad (24)$$

Let c(n) be a phase correction function that we would like to match to the atmospheric noise, i.e., by some means make

$$c(n) = \Theta(n)_{noise}.$$

If $c(n) = \Theta(n)_{noise}$, then

$$R(s) = \sum_{n} A(n)\exp\left\{i\left[\frac{2\pi(n-s)^2(\delta x)^2}{R} + \Theta(n) - c(n)\right]\right\} \qquad (25)$$

yields the desired system output. We must first devise some means of computing c(n), however.

Consider the effect of the atmosphere on the beam pattern (system response to a single target); peak gain is reduced, undesired side lobes are introduced, the main lobe is spread out and there may be pointing error. Intuitively one would like to define the criterion function in such a way as to put a premium on increasing the gain, narrowing the beam and reducing sidelobes. Beam pointing error could be considered as a separate problem. One possible criterion function which does this is maximizing the variance of the magnitude of the system output, R(s). Maximum variance of $|R(s)|$ is also consistent with the intuitive notion of maximum sharpness.

The variance of the magnitude of the system output, R(s) can be written as

$$V = \frac{1}{B} \sum_{s=-\frac{B}{2}}^{\frac{B}{2}} |R(s)|^2 - \left[\frac{1}{B} \sum_{s=-\frac{B}{2}}^{\frac{B}{2}} |R(s)| \right]^2, \tag{26}$$

where R(s) is defined by equation (25).

It would then seem to be just a simple matter of adjusting c(n) to obtain the maximum variance, V_{max}, and c(n) would then be optimum. However, no improvement (increase in V) will be noted if c(n) is adjusted over only a small subset of the array elements at a time. It must be adjusted simultaneously over all of the elements used in processing an interval and in such a way as to maintain a continuous curve for c(n). One is led naturally, then, to consider using a Fourier series (or possibly a series of orthogonal polynomials) for c(n). Since coefficients for the Fourier series must be computed, only a limited number of terms can be included. We can write the series approximation to c(n) as

$$c(n) = \sum_{m=1}^{K} a_m \cos\left(\frac{2\pi(mn + b_m)}{2N + B}\right),$$

which is the same approximation that was used for the atmospheric noise in Chapter 3.

Equation (25) then becomes

$$R(s) = \sum_n A(n) \exp\left\{ i \left[\frac{2\pi(n-s)^2(\delta x)^2}{R} + \Theta(n) - \sum_{m=1}^{K} a_m \cos\left(\frac{2\pi(mn + b_m)}{2N + B}\right) \right] \right\}. \tag{27}$$

The criterion for establishing values for a_m and b_m is to adjust them until the variance defined by equation (26) is maximized.

3. COMPUTER SIMULATION

In order to run completely controlled experiments to evaluate the effectiveness of determining c(n) by adjusting the a_m and b_m to maximize the variance of $|R(s)|$, the complete system (including targets) was modeled on a CDC 1604 computer. The simulation was done in essentially two parts; the received signals from multiple targets at range R were computed and recorded as data, then this data was used as the input to the processor.

A. GENERATION OF THE RECEIVED SIGNALS

At range R from the synthetic array, data for multiple point targets was generated. Pseudo random numbers were used for target amplitude, spacing between targets and phase of the targets. Targets were placed along a line at range R throughout the beam of the coherent radar — for all of its positions, nδx, over a region corresponding to 4Nδx. The 4N "received" signals were computed from

$$s(n\delta x) = A(n)\exp\left[i\Theta(n)\right]$$

$$= \sum_{k=\left[n-\frac{R\phi}{2\delta x}\right]}^{\left[n+\frac{R\phi}{2\delta x}\right]} A(k)\exp\left\{-i2\pi\left[\frac{(n-k)^2(\delta x)^2}{R} + P(k)\right]\right\} \qquad (28)$$

where ϕ = coherent radar beamwidth in radians,

A(k) = target amplitude received from location k and

P(k) = phase of target (reflects location of phase center).

These 4N recorded signals, s(nδx), were processed according to

$$R(s) = \sum_{n=s-N}^{s+N} A(n)\cos^2\left(\frac{\pi(n-s)}{2N}\right)\exp\left\{i\left[\frac{2\pi(n-s)^2(\delta x)^2}{R} + \Theta(n)\right]\right\}, \qquad (29)$$

to obtain the "no noise" system output, cosine squared weighting and focused at range R and $s\delta x$.

Pseudo random numbers were filtered using an integrating type filter to obtain 4N numbers to be used to simulate the atmospheric phase noise. The "bandwidth" of the filter was selected to yield the phase correlation length desired for the particular simulation. The peak to peak phase noise desired was obtained by multiplying the 4N numbers by a constant. These 4N numbers, simulating atmospheric phase noise, were then added to the $\Theta(n)$, forming a new $s(n\delta x)$. The system output was again computed, using equation (29), to obtain the perturbed output. By proceeding in this fashion, data is obtained that can be used in evaluating the effectiveness of the processor. The computed $c(\bar{n})$ can be compared to the actual noise used and the final system output, using the computed $c(n)$, to both the "no noise" and with noise system outputs.

B. COMPUTING c(n)

The received signals, $s(n\delta x)$, with the noise included were processed according to equations (27) and (26) as described in Section 2. The variance of $|R(s)|$, since it is used as the criterion, must be evaluated each time new values for the a_m and b_m are tried. This takes time so only a limited number of harmonics can be used (six were finally used). There is also some interdependence between the harmonics which precludes the possibility of "taking them out" completely one at a time. An iterative technique was decided upon wherein the initial variance is first computed and then the processor starts out with the first harmonic. A low value for a_1 is set and then b_1 is varied through a range equivalent

to 360 degrees to locate the phase angle which yields the highest variance. If the maximum variance so located is higher than the initial variance, it replaces the initial variance as a standard for comparison. The corresponding value for b_1, together with the value a_1, is used in the cosine as the first approximation to c(n). The second harmonic is then treated in similar fashion to find the maximum variance value for b_2. If the maximum variance here is greater than the standard for comparison (the highest variance previously obtained), then the a_2 and b_2 are used to add to the approximation to c(n) and a new standard is set corresponding to the maximum variance achieved here. This procedure is repeated on through the K^{th} harmonic, then the cycle through harmonics one to K is repeated. The processor continues to cycle through the harmonics in this fashion until no further improvement (increase in variance of $|R(s)|$) can be obtained. The processor has now made its best estimate for c(n).

It was found, during early cycles of the processor, that on any given cycle it may or may not locate the correct phase value for a particular harmonic, but that over a number of cycles it would average out to the correct one. This indicated that it was not necessary, nor desirable, to check closely spaced phase points — values of b_m equivalent to 30 degree increments were adequate. Enough cycles to allow the phase to average out were obtained by setting the value of a_m equal to 0.01 λ.

C. PARAMETERS OF THE SIMULATION

To form the synthetic array the vehicle (normally an aircraft) would travel a straight line path at velocity, v, carrying the coherent

radar with an antenna beamwidth, ϕ. It is common (although not necessary) to have the antenna pointed normal to the path of the vehicle. A value of 0.05 radians was used for ϕ in the simulation — it being considered a typical value. Based on this ϕ, we can arrive at other parameters for our simulation. The maximum doppler frequency, $(fd)_{max}$, is

$$(fd)_{max} = \frac{2v \sin(\frac{\phi}{2})}{\lambda}$$

$$\simeq \frac{v\phi}{\lambda},$$

since $\sin(\frac{\phi}{2}) \simeq \frac{\phi}{2}$, for small ϕ. Using the sampling theorem, we find that the minimum pulse repetition frequency, PRF_{min}, required is

$$PRF_{min} = \frac{2v\phi}{\lambda}.$$

The pulse repetition time, PRT, is 1/PRF, or

$$PRT_{max} = \frac{\lambda}{2v\phi}.$$

The distance traveled between pulses of the coherent radar, δx, becomes

$$\delta x = v(PRT),$$

or

$$\delta x_{max} = \frac{\lambda}{2\phi}$$

$$= 10\lambda$$

using $\phi = 0.05$ radians. This was the value used in the simulation.

In the interest of conserving computer time, the length of the array and the range to the targets were scaled down, while the multiplicative noise was not. A value for N of 100 was used and most of the computer runs were made with a range, R, of $80{,}000\lambda$.

A considerable number of computer runs was made with different

parameters for the noise and targets. All were made using a focused processor, part with cosine squared weighting and part with uniform weighting used in the computation of $\dot{c}(n)$. Uniform weighting proved to be the best. Different methods of computing the a_m and b_m of the approximation to the phase noise were also tried, but the best method was the one described in Section B.

It was determined early in the computer simulation runs that it would be desirable to find some method of decreasing the processing time. It seemed reasonable that if the higher frequencies in the received signal could be filtered out prior to processing that it would be possible to use just some fraction of the elements in the processing. The highest frequency contributed from the interval being processed is less than one-fifth of the highest doppler frequency being received. By filtering it was possible to allow the processor to operate with every fifth element, resulting in a five-fold decrease in processing time. The pre-filter used was an integrating type. A small number, L, of the recorded signal returns, $s(n\delta x)$, was steered to "look" toward the center of the region to be processed, summed with cosine squared weighting and recorded as $p(n\delta x)$ of a new filtered array. This process was repeated, each time shifting the L recorded returns by an amount δx, until $2N + B$ (the number of elements required in a processing interval) of the $p(n\delta x)$ were computed. Mathematically the pre-filtering operation is

$$p(n\delta x) = \sum_{t=n-\frac{L}{2}}^{n+\frac{L}{2}} A(t)\cos^2\left(\frac{\pi(n-t)}{L}\right)\exp\left\{i\left[\frac{4\pi(\delta x)^2(n-t)n}{R} + \Theta(t)\right]\right\}, \quad (30)$$

where L is even. A value of L equal to 30 was used. Such a filter does

not have sharp cut-off characteristics. The magnitude of the system output is down to about 50 percent at the ends of the processed interval, relative to the center value, when such a pre-filter is used. It decreases in approximately exponential fashion outside the interval.

It must be emphasized that the only reason a pre-filter was used was to decrease the processing time.

Representative results of the computer runs are shown as Figures 18 through 31. System outputs for "no noise", with noise and after noise processing are shown. In the following figure, the original phase noise used and the residual noise after processing are presented, the residual noise being found by subtracting the approximation, c(n), from the original phase noise.

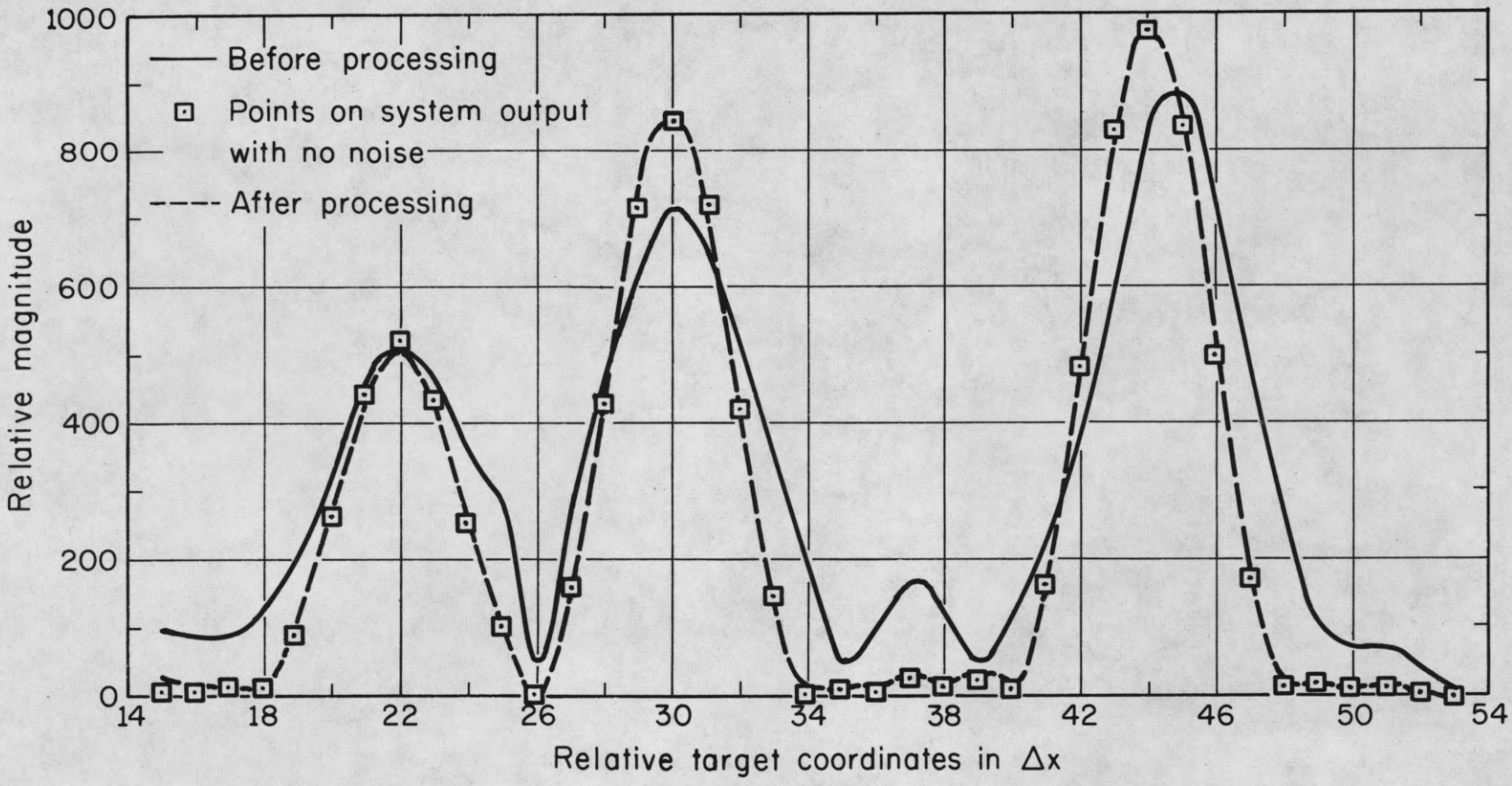

Figure 18. System Output Before and After Noise Processing, Run 1

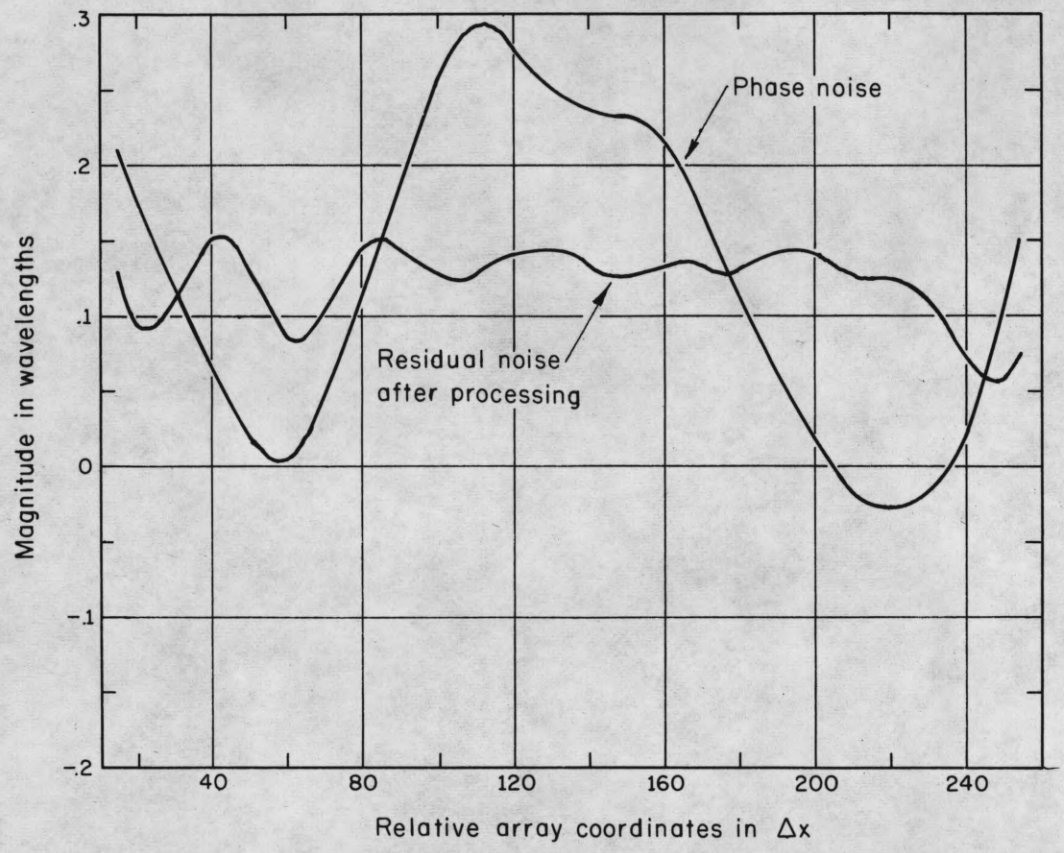

Figure 19. Phase Noise and Residual Phase Noise After Processing, Run 1

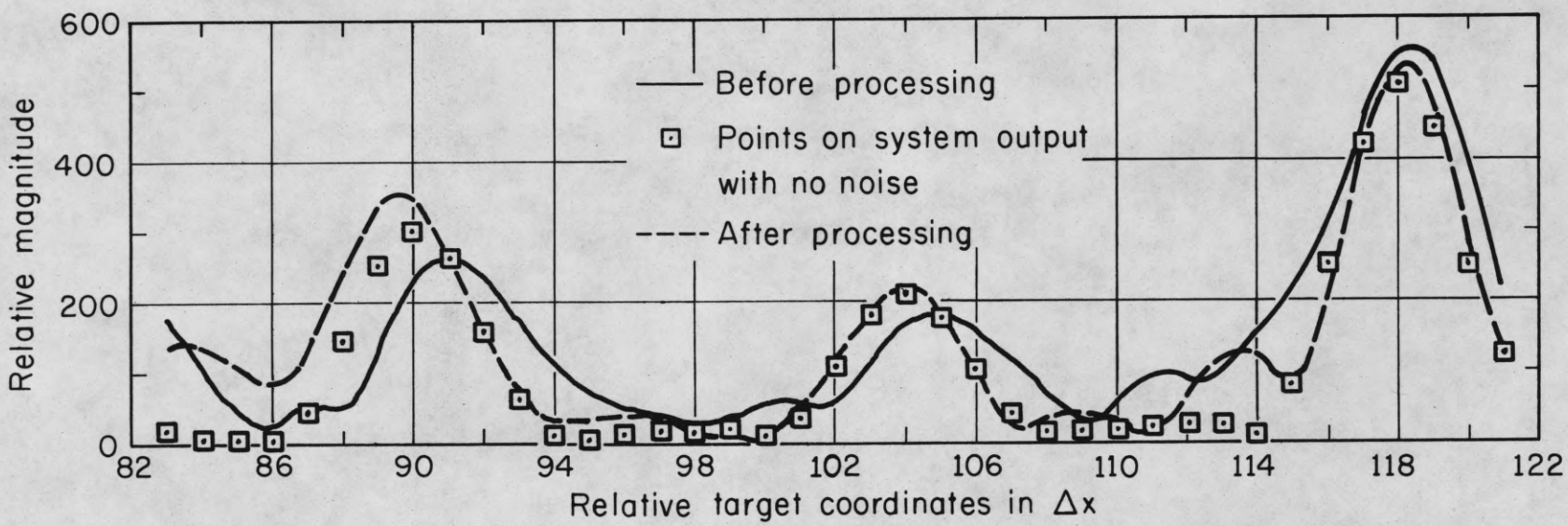

Figure 20. System Output Before and After Noise Processing, Run 5

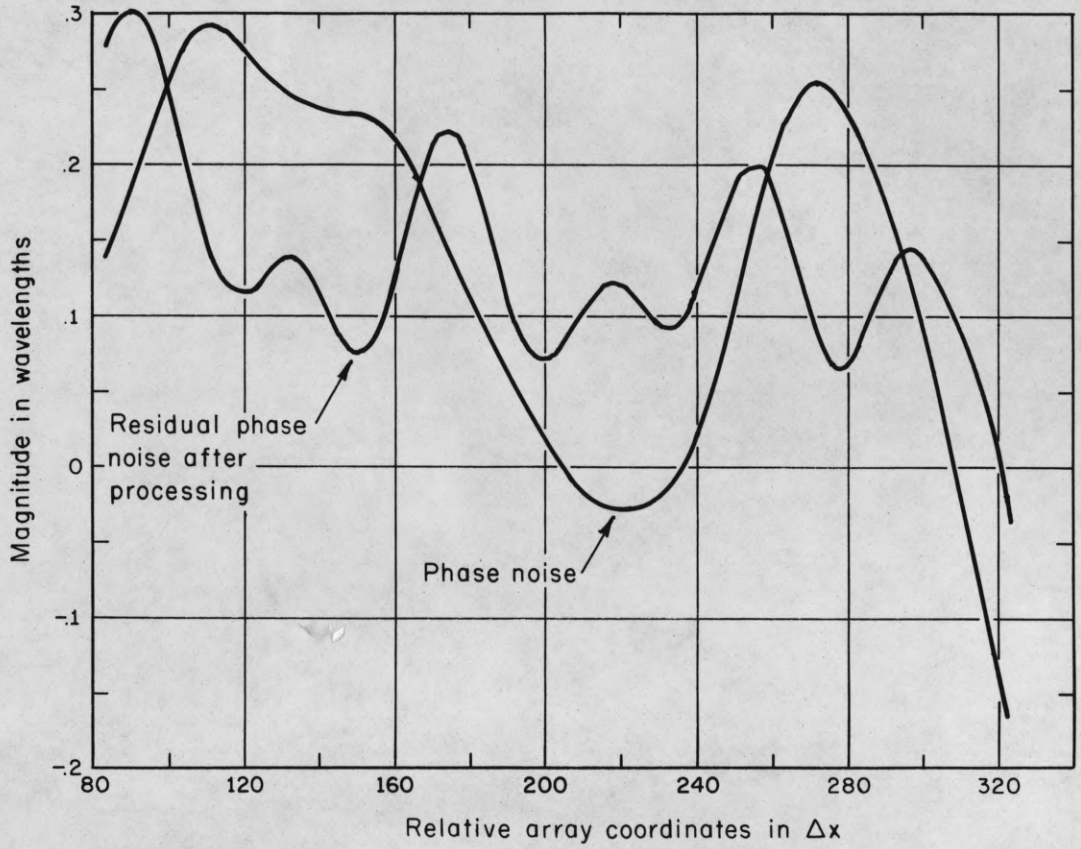

Figure 21. Phase Noise and Residual Phase Noise After Processing, Run 5

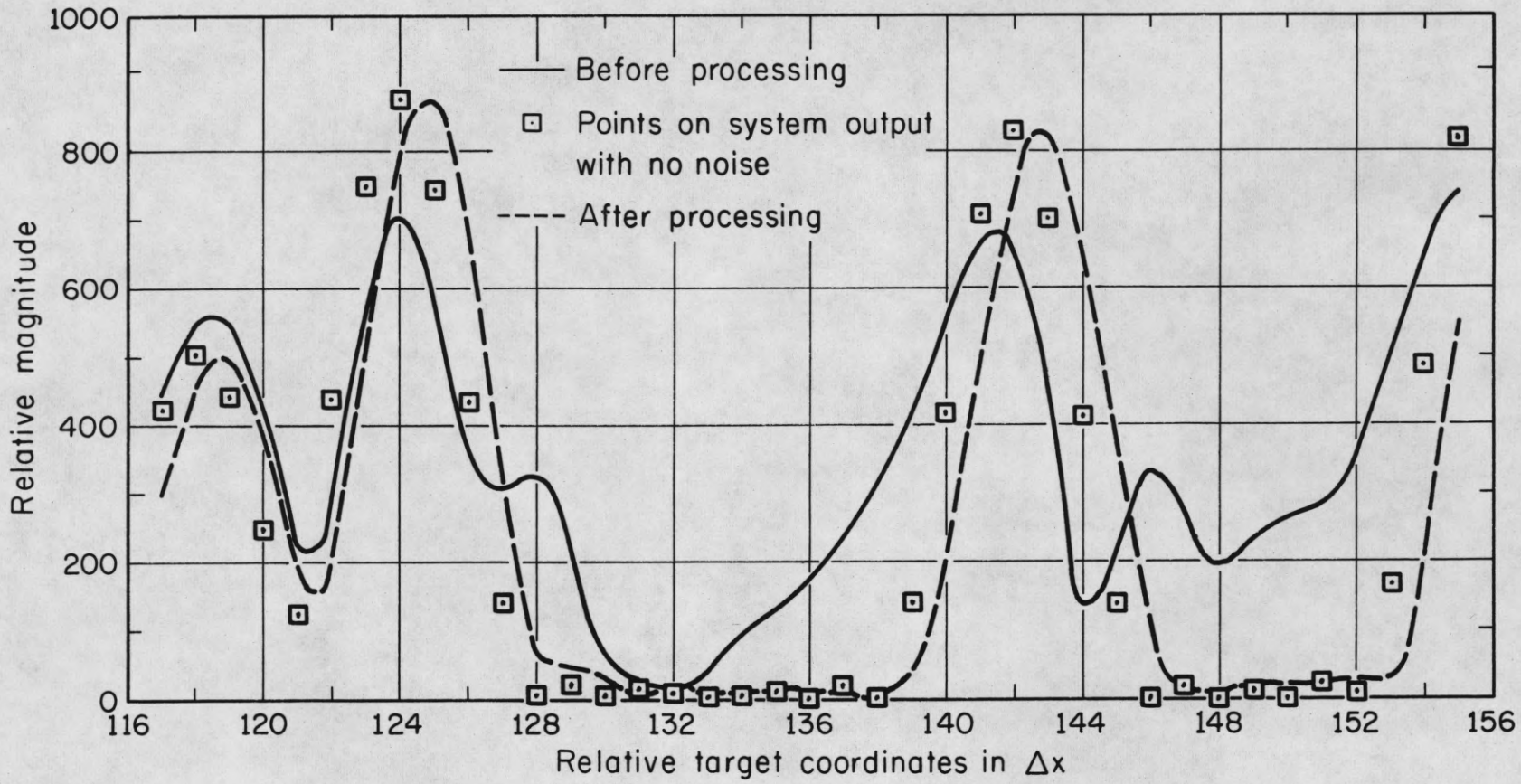

Figure 22. System Output Before and After Noise Processing, Run 6

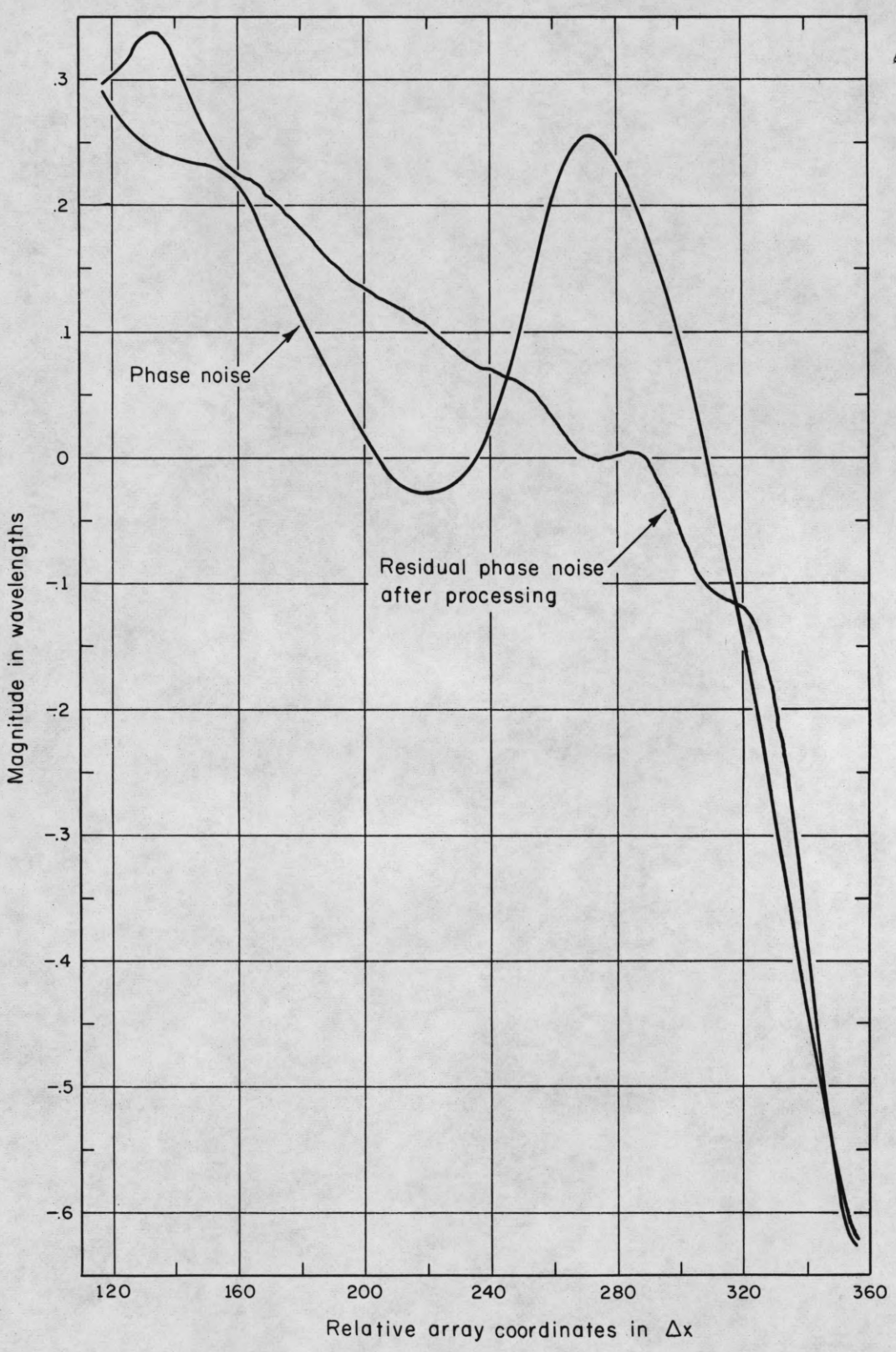

Figure 23. Phase Noise and Residual Phase Noise After Processing, Run 6

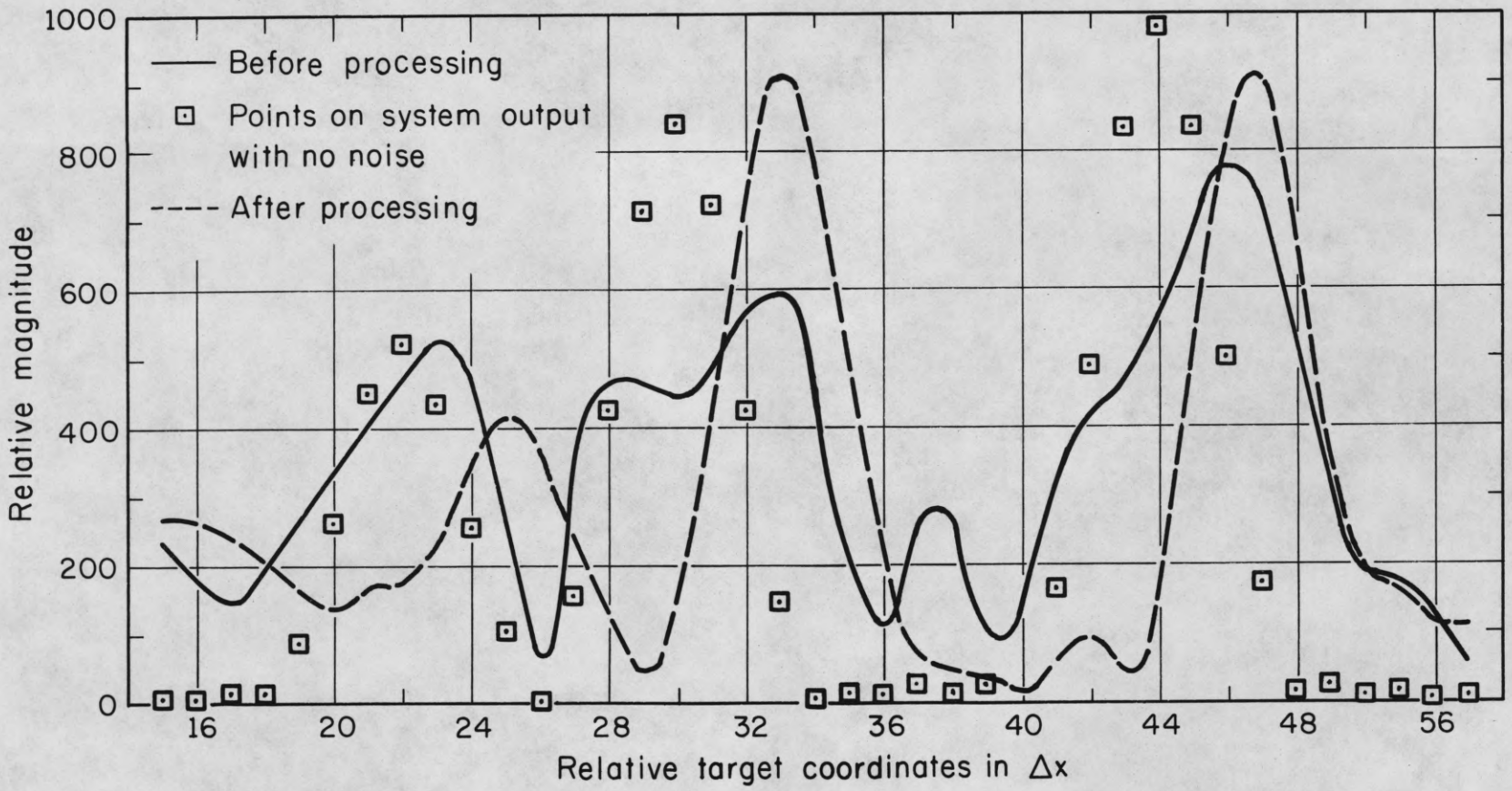

Figure 24. System Output Before and After Noise Processing, Run 7

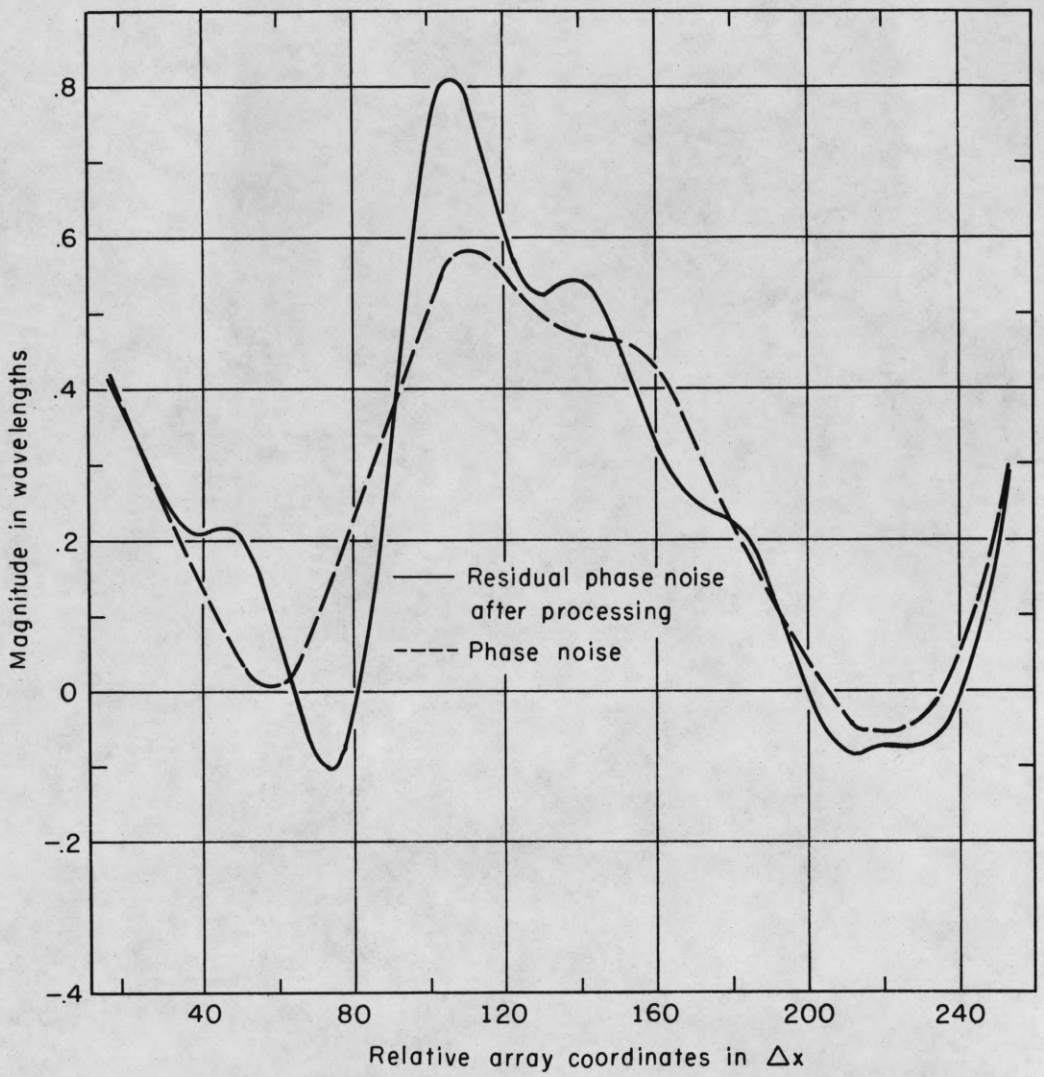

Figure 25. Phase Noise and Residual Phase Noise After Processing, Run 7

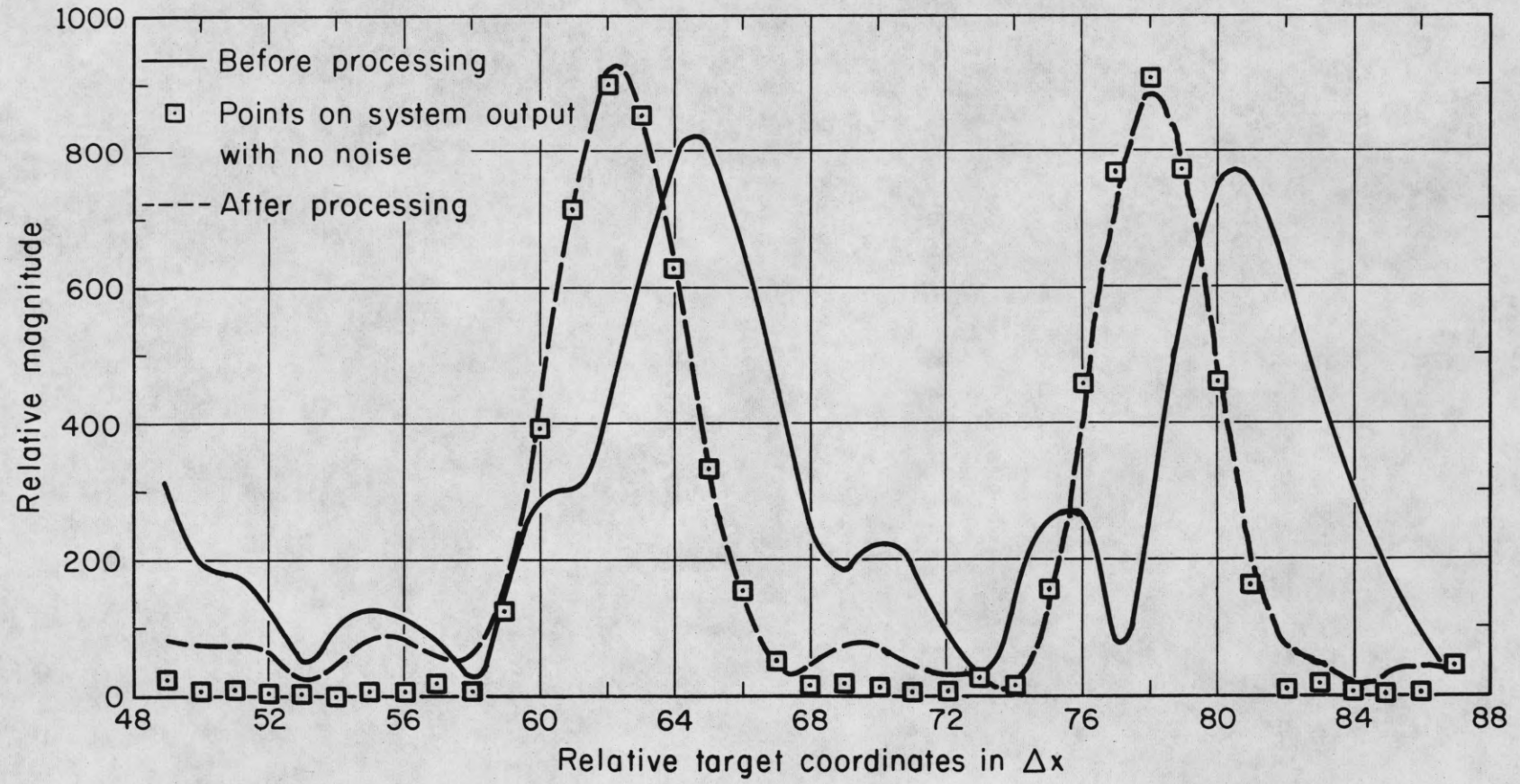

Figure 26. System Output Before and After Noise Processing, Run 8

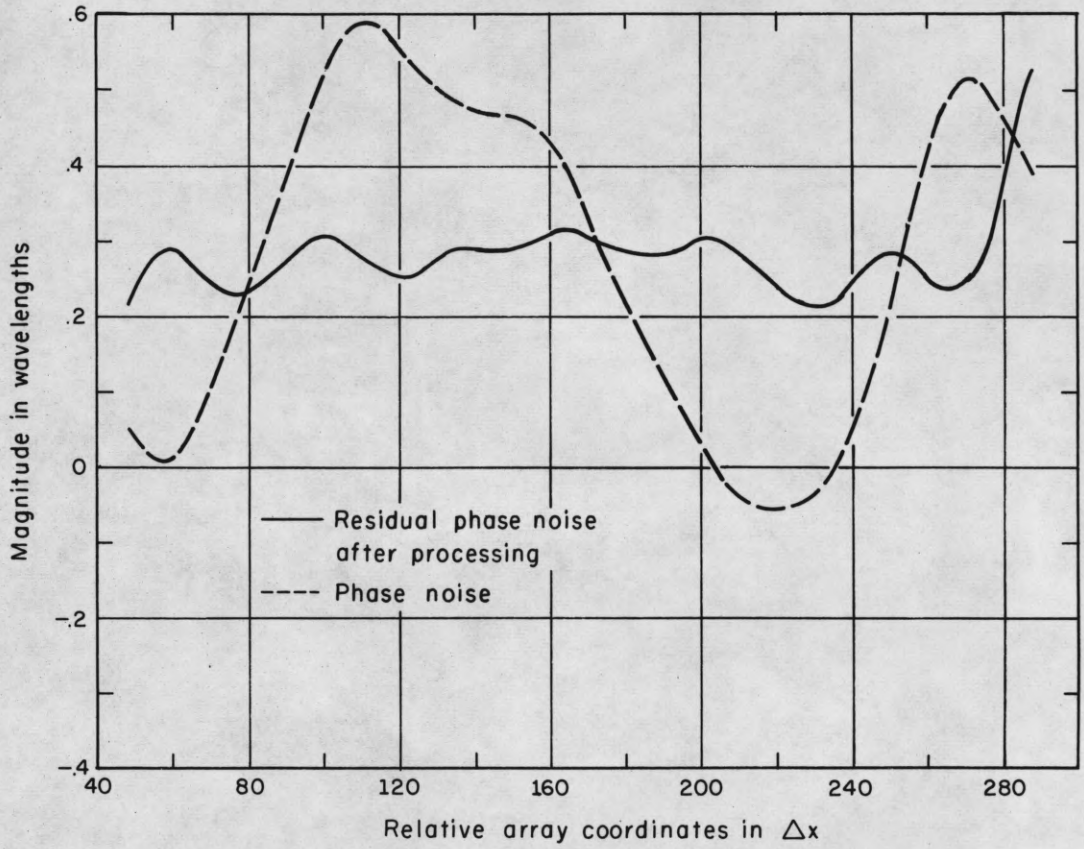

Figure 27. Phase Noise and Residual Phase Noise After Processing, Run 8

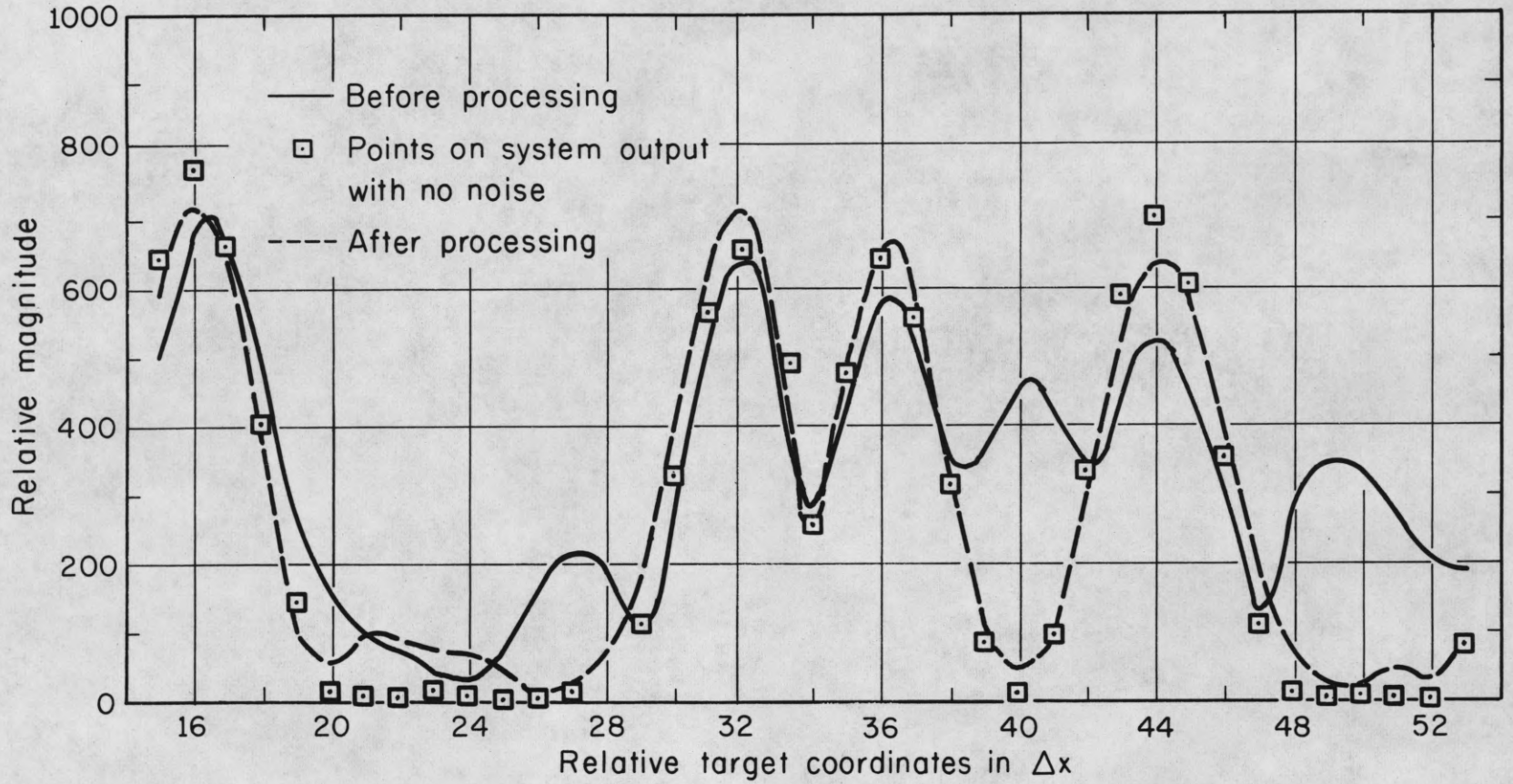

Figure 28. System Output Before and After Noise Processing, Run 10

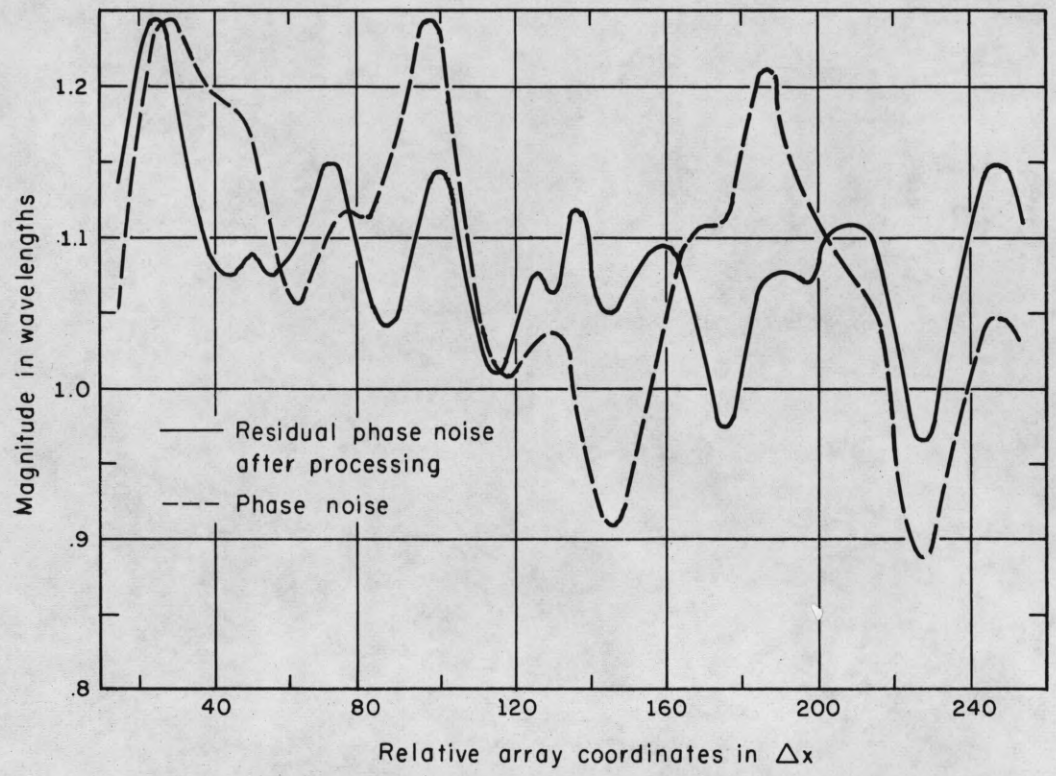

Figure 29. Phase Noise and Residual Phase Noise After Processing, Run 10

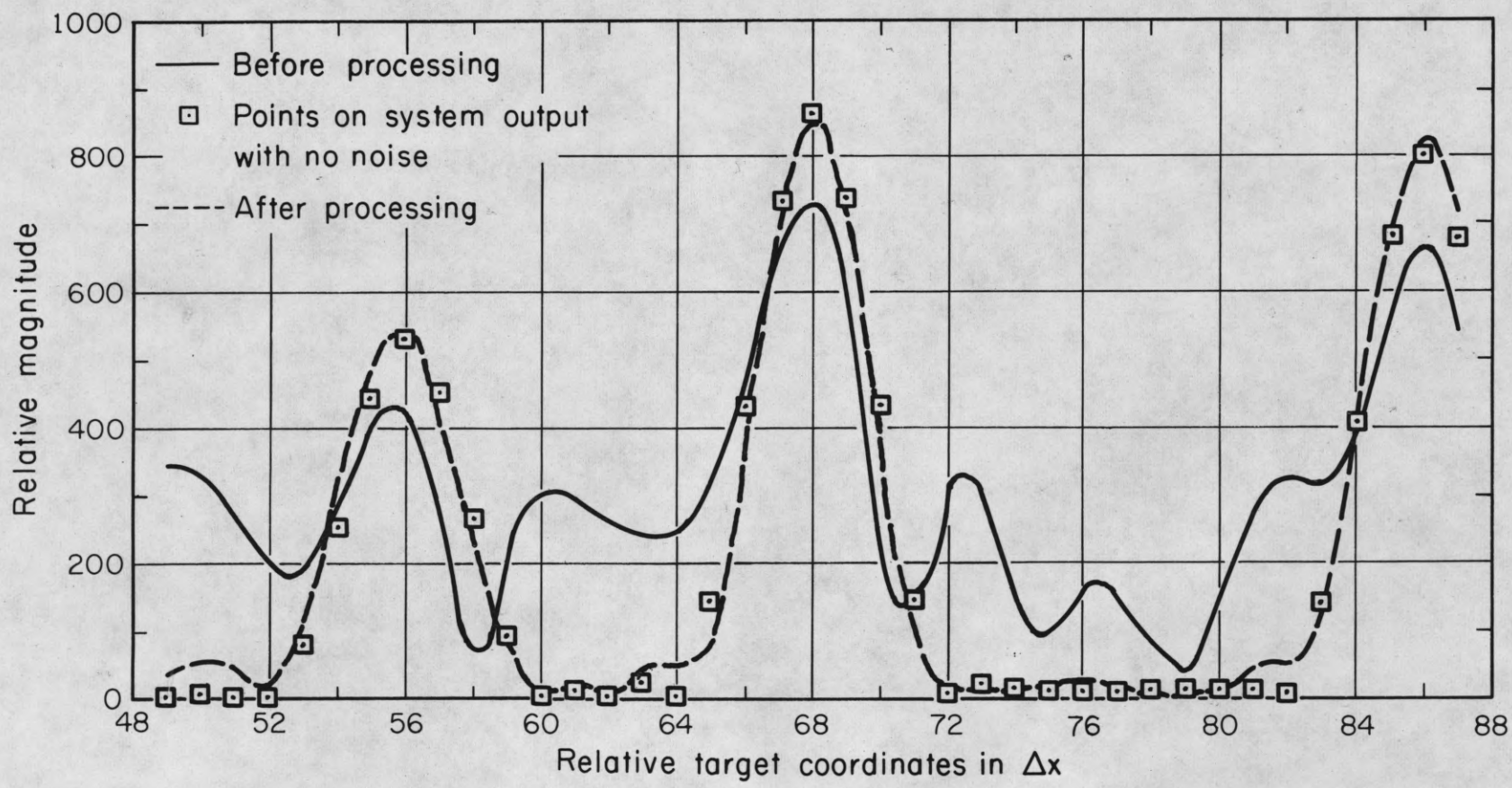

Figure 30. System Output Before and After Noise Processing, Run 14

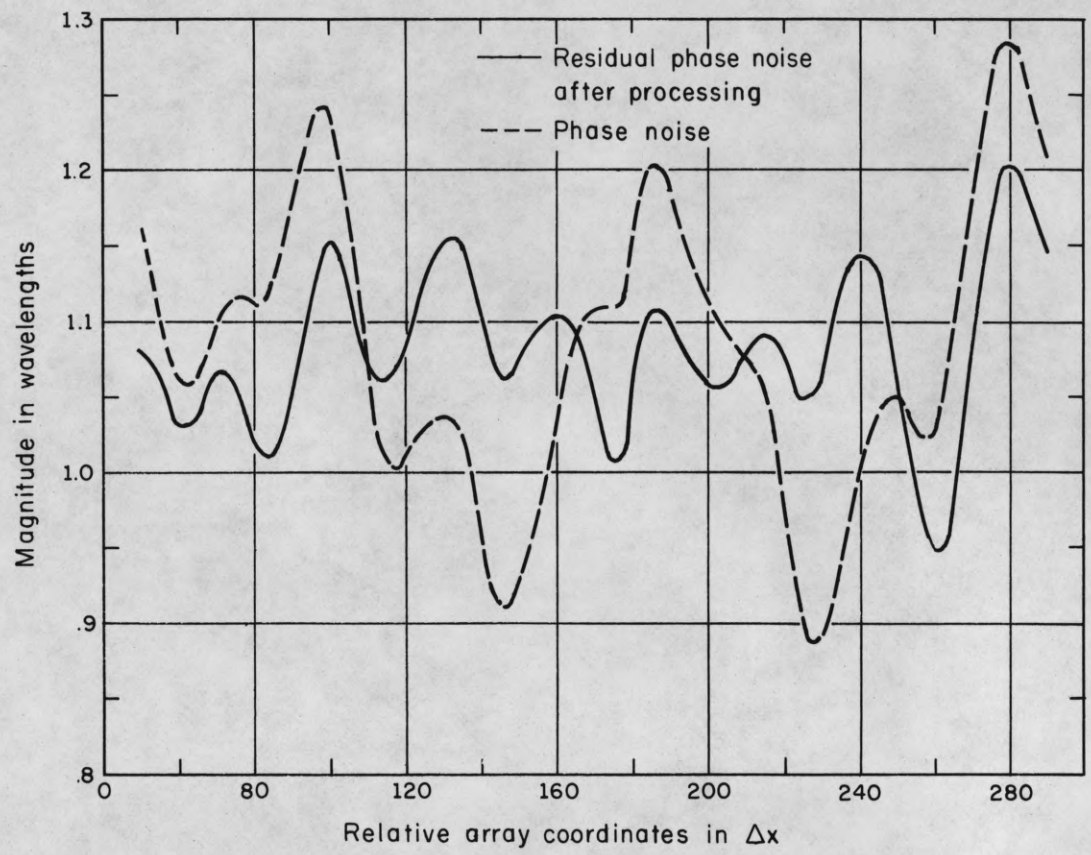

Figure 31. Phase Noise and Residual Phase Noise After Processing, Run 14

V. DISCUSSION OF RESULTS

As might be expected, the processor described in the previous chapter is effective only over some region of the possible parameters. Figures 18 through 31 were chosen to illustrate, in a sense, the boundaries within which it might be expected to perform satisfactorily. In all cases illustrated some improvement in the system output is noted. However, the estimate of the phase noise, c(n), was not always the best. It was found that when the amplitude of the noise was less than approximately two radians peak to peak and with negligible frequency content higher than that used in the processor (sixth harmonic), then the c(n) found was a good approximation to the phase noise about three-fourths of the time. Under these conditions the processor may, however, leave in a steering slope. Figures 18 and 19 are representative of the runs yielding a good approximation to the phase noise, while Figures 22 and 23 illustrate a relatively good approximation, but with a residual steering slope. Figures 20 and 21 illustrate a run which, from the characteristics of the noise used, should have yielded a better noise approximation, c(n), than was obtained. It is believed that this resulted due to the magnitude characteristic in the processing interval, caused by the use of the pre-filter, in combination with this particular set of target parameters. However, it does lead one to consider possible means of allowing the processor to avoid using a poor estimate of the phase noise for c(n).

Figures 28 through 31 illustrate the behavior when the phase noise used has significant "frequency" content higher than that used in the processor. Even if the processor was allowed to use higher harmonics, it could not be expected to function as well on noise with significant

"high frequency" content. Undesired side lobes caused by the phase noise move further from the main lobe as the phase noise "frequency" is increased, as is illustrated in Figures 3 through 14. The phase noise, through the side lobes created, may cause an interaction between targets. It is possible that the interaction may have such an effect upon the variance of $|R(s)|$ as to allow the processor to proceed toward a false maximum for the variance, resulting in a poor approximation for c(n). The results of a number of runs show that marginal results are obtained when the "frequency" content of the phase noise is similar to that of Figures 29 and 31.

It would be expected, based on the degree of beam pattern distortion shown in Figures 3 through 14, that the processor would not function well on much higher phase noise levels than approximately two radians peak to peak. Trial runs were made with peak to peak levels near four radians to illustrate the behavior. The results of two of these runs are shown in Figures 24 through 27. They represent the relatively good results that occurred on approximately one-half of the high level runs. Figures 24 and 25 deserve special comment. On this run the processor found an approximation, c(n), that converted the original phase noise into essentially two regions of nearly the same slope and separated by a step in phase of approximately one wavelength. A phase step of exactly one wavelength has no effect on the system output. The net effect was that the resulting system output was quite good but with a pointing error.

When the noise is such that most of the time a good approximation

to the phase noise is obtained, then it should be possible to modify the processor in such a way as to allow it to avoid using a poor approximation for c(n), in any given interval. One would not expect the correlation nor amplitude characteristic of the atmospheric turbulence phase noise to change significantly from one processing interval to the next. If the processor is modified such that it "remembers" such statistics for a time, then it can compare them over several processing intervals. If one interval is encountered that deviates significantly, then it would be an indication that more processing should be done. There are two possibilities for obtaining a better approximation for c(n) for such an interval.

It will be noted that if the interval is small compared to the length of the array, which it will be, then most of the array elements used for the interval in question were also used for the intervals to either side. Since we have assumed that the processed interval is small compared to the correlation length, then the phase noise must be quite similar to that of the adjacent intervals and the processor could just use the appropriate portions of the c(n) obtained for the adjacent intervals as the c(n) for the interval in question.

Alternatively we might just have the processor try processing for a slightly different range such that a new set of targets are used in the processing. Runs were made which do show the processor is somewhat dependent upon the target parameters, so this procedure might yield a better approximation for c(n). In fact, if processing time would allow it, the processor might be allowed to process a number of ranges for each interval and then use the average approximation found as c(n). A good approximation for c(n) would be more probable if this were done.

VI. CONCLUSIONS AND RECOMMENDATIONS FOR FURTHER WORK

1. CONCLUSIONS

This study has developed a realistic model of the atmospheric turbulence effects on a synthetic aperture radar system. It proved useful in a deterministic, rather than statistical, approach to showing what the effects of atmospheric turbulence would be on a synthetic aperture system.

The processing technique developed demonstrates the feasibility of processing the recorded radar data to remove the effects of atmospheric turbulence. With such processing, longer useful synthetic arrays could be formed, thus improving resolution. However, since the processing described in this study is only effective over a somewhat limited region of phase noise parameters (as was pointed out in the discussion of results), we cannot say with certainty that we have removed the atmospheric limitation on resolution completely.

It would appear that the processing technique described here might also be effective in removing some of the other sources of phase errors in synthetic systems, since they may have characteristics similar to those assumed for the atmospheric turbulence.

2. RECOMMENDATIONS FOR FURTHER WORK

There are several areas that should be investigated to extend and/or verify the usefulness of this study. The model of the atmospheric turbulence was developed as the best "fit" to available data. Experiments should be performed that investigate the effects of the atmosphere more fully on frequencies of interest in synthetic radar work.

This study tacitly assumed an infinite signal-to-noise ratio for the signals being processed. Since the received signals would be corrupted to some extent by additive Gaussian noise, the effect on the processor should be investigated. Target scintillation, caused by a shift in phase center with aspect angle, was not investigated. Its effect on the processor should also be considered.

Doing all of the processing via a digital computer as was done in this study may not be optimum, from the standpoint of processing time. Analog or optical processing may prove to be much faster. Optical processing would have the advantage that a significant range interval could be processed simultaneously with the azimuth processing. That is, processing in two dimensions could proceed at the same time.[7] This would require a modification of the variance criterion, in that the processor would then use the variance of the magnitude of the system output in two dimensions. This would automatically make the approximation to the phase noise the average over some range interval and hence more probable that the approximation found is good.

BIBLIOGRAPHY

1. Angulo, C. M. and Ruina, J. P., "Antenna Resolution as Limited by Atmospheric Turbulence", Coordinated Science Laboratory Report R-96, University of Illinois, Urbana, Illinois (July, 1957).

2. Bendat, J. S., Principles and Applications of Random Noise Theory, John Wiley & Sons, Inc., New York (1958).

3. Bitzer, D. L., "Signal Amplitude Limiting and Phase Quantization in Antenna Systems", Doctoral Thesis, University of Illinois, Urbana, Illinois (December, 1959).

4. Cramond, W. R. and Thorn, D. C., "An Approach to Azimuth Angle Refraction Corrections", Engineering Experiment Station Report EE-72, University of New Mexico, Albuquerque, New Mexico (April, 1962).

5. Cramond, W. R., Leeman, J. E. and Thorn, D. C., "Radar Elevation Angle Errors and Refraction Corrections", Engineering Experiment Station Report EE-79, University of New Mexico, Albuquerque, New Mexico (September, 1962).

6. Cutrona, L. J., Vivian, W. E., Leith, E. N. and Hall, G. O., "A High-Resolution Radar Combat-Surveillance System", IRE Transactions on Military Electronics MIL-5, 127 (April, 1961).

7. Cutrona, L. J., Leith, E. N. and Porcello, L. J., "Filtering Operations Using Coherent Optics", Proceedings of the National Electronics Conference 15, 262 (October, 1959).

8. Cutrona, L. J. and Hall, G. O., "A Comparison of Techniques for Achieving Fine Azimuth Resolution", IRE Transactions on Military Electronics MIL-6, 119 (April, 1962).

9. Deam, A. P. and Fannin, B. M., "Phase Difference Variations in 9,350 Megacycle Radio Signals Arriving at Spaced Antennas", Proceedings of the IRE 40, 1402 (October, 1955).

10. Dutton, E. J. and Thayer, G. O., "Techniques for Computing Refraction of Radio Waves in the Troposphere", Technical Documentary Report No. ESD-TDR-62-289, Electronic Systems Division, Air Force Systems Command, L. G. Hanscom Field, Bedford, Massachusetts (October, 1962).

11. Greene, C. A. and Moller, R. T., "The Effect of Normally Distributed Random Phase Errors on Synthetic Array Gain Patterns", IRE Transactions on Military Electronics MIL-6, 130 (April, 1962).

12. Herbstreit, J. W. and Thompson, M. C., "Measurements of the Phase of Radio Waves Received over Transmission Paths with Electrical Lengths Varying as a Result of Atmospheric Turbulence", Proceedings of the IRE 40, 1391 (October, 1955).

13. McCord, H. L., "The Equivalence Among Three Approaches to Deriving Synthetic Array Patterns and Analyzing Processing Techniques", IRE Transactions on Military Electronics MIL-6, 116 (April, 1962).

14. Muchmore, R. B. and Wheelon, A. D., "Line-of-Sight Propagation Phenomena — I. Ray Treatment", Proceedings of the IRE 40, 1437 (October, 1955).

15. Schlesinger, R. J., Principles of Electronic Warfare, Prentice Hall, Inc., New Jersey (1961).

16. Sherwin, C. W., Ruina, J. P. and Rawcliffe, R. D., "Some Early Developments in Synthetic Aperture Radar Systems", IRE Transactions on Military Electronics MIL-6, 111 (April, 1962).

17. "Refraction Corrections for Tracking Data", Western Development Laboratories Report No. WDL-TR1903, Philco Corporation, Palo Alto, California (September, 1962).

VITA

Dale M. Diamond was born February 18, 1929 in Springville, Utah. He is married and has two children, a son and a daughter.

In the Fall of 1947, he enlisted in the United States Air Force where he attended the Radar School at Keesler A. F. B., Mississippi. He spent the remainder of his four years in the Air Force at the Radar School as an instructor. Upon discharge from the Air Force he spent one year as a Philco Technical Representative at Aberdeen Proving Ground, Maryland, where he taught radar in the Ordnance School. The following year was spent as a field engineer for Bendix Radio Corporation where he was the factory representative at an Early Warning Radar Station in the state of Washington.

His academic training began at the University of Utah in 1953, where he received a B. S. E. E. degree in 1957. Among the honors received at the University of Utah, he was voted the "Outstanding Senior Engineering Student". Upon graduation in 1957, he went to work for Bell Telephone Laboratories in Murray Hill, New Jersey. While there he attended classes at New York University as part of the Bell Telephone Laboratories Communication and Development Training (CDT) Program. In 1958, he went to work for Space Technology Laboratories at their space tracking station in Hawaii, taking over the management of the station in 1959.

In 1960, he became a student at the University of Illinois where, in addition to his academic work, he was a half-time research assistant at the Coordinated Science Laboratory. He received a Master's degree in Electrical Engineering from the University of Illinois in 1961. His doctoral dissertation was completed while working as a research

associate at the Coordinated Science Laboratory. Since being employed by the Coordinated Science Laboratory in 1960, a major portion of his research activity has been with the PLATO (a digital computer-controlled teaching system) project.

In addition to the above mentioned, he also worked the summer of 1955 as a field engineer for Bendix Radio Corporation and the summer of 1956 as an electronics engineer for Convair in Pomona, California.

He is a member of the IEEE, Tau Beta Pi, Eta Kappa Nu, Phi Kappa Phi and Theta Tau.

DISTRIBUTION LIST AS OF JULY 12, 1963

1 Director
Air University Library
Maxwell Air Force Base, Alabama
Attn: CR-4803a

1 Redstone Scientific Information Center
U.S. Army Missile Command
Redstone Arsenal, Alabama

1 Electronics Research Laboratory
University of California
Berkeley 4, California

2 Hughes Aircraft Company
Florence and Teale
Culver City, California
Attn: N. E. Devereux
Technical Document Center

3 Autonetics
9150 East Imperial Highway
Downey, California
Attn: Tech. Library, 3041-11

1 Dr. Arnold T. Nordsieck
General Motors Corporation
Defense Research Laboratories
6767 Hollister Avenue
Goleta, California

1 University of California
Lawrence Radiation Laboratory
P. O. Box 808
Livermore, California

1 Mr. Thomas L. Hartwick
Aerospace Corporation
P. O. Box 95085
Los Angeles 45, California

1 Lt. Colonel Willard Levin
Aerospace Corporation
P. O. Box 95085
Los Angeles 45, California

1 Professor Zorab Kaprelian
University of Southern California
University Park
Los Angeles 7, California

1 Sylvania Electronic Systems - West
Electronic Defense Laboratories
P. O. Box 205
Mountain View, California
Attn: Documents Center

1 Varian Associates
611 Hansen Way
Palo Alto, California
Attn: Dr. Ira Weissman

1 Huston Denslow
Library Supervisor
Jet Propulsion Laboratory
California Institute of Technology
Pasadena, California

1 Professor Nicholas George
California Institute of Technology
Electrical Engineering Department
Pasadena, California

1 Space Technology Labs., Inc.
One Space Park
Redondo Beach, California
Attn: Acquisitions Group
STL Technical Library

2 Commanding Officer and Director
U.S. Naval Electronics Laboratory
San Diego 52, California
Attn: Code 2800, C. S. Manning

92052

1 Commanding Officer and Director
U.S. Navy Electronics Laboratory
San Diego 52, California
Attn: Library

1 Office of Naval Research Branch Office
1000 Geary Street
San Francisco, California

1 The RAND Corporation
1700 Main Street
Santa Monica, California
Attn: Library

1 Stanford Electronics Laboratories
Stanford University
Stanford, California
Attn: SEL Documents Librarian

1 Dr. L. F. Carter
Chief Scientist Air Force
Room 4E-324, Pentagon
Washington 25, D. C.

1 Mr. Robert L. Feik
Associate Director for Research
Research and Technology Division
AFSC
Bolling Air Force Base 25, D. C.

1 Captain Paul Johnson (USN-Ret)
National Aeronautics and Space
Administration
1520 H Street, N. W.
Washington 25, D. C.

1 Major Edwin M. Myers
Headquarters USAF (AFRDR)
Washington 25, D. C.

1 Dr. James Ward
Office of Deputy Director
(Research and Info)
Department of Defense
Washington 25, D. C.

1 Dr. Alan T. Waterman
Director, National Science Foundation
Washington 25, D. C.

1 Mr. G. D. Watson
Defense Research Member
Canadian Joint Staff
2450 Massachusetts Ave., N. W.
Washington 8, D. C.

1 Mr. Arthur G. Wimer
Chief Scientist
Air Force Systems Command
Andrews Air Force Base
Washington 25, D. C.

1 Director, Advanced Research
Projects Agency
Washington 25, D. C.

1 Air Force Office of Scientific Branch
Directorate of Engineering Sciences
Washington 25, D. C.
Attn: Electronics Division

1 Director of Science and Technology
Headquarters, USAF
Washington 25, D. C.
Attn: AFRST-EL/GU

1 Director of Science and Technology
AFRST - SC
Headquarters, USAF
Washington 25, D. C.

1 Headquarters, R & T Division
Bolling Air Force Base
Washington 25, D. C.
Attn: RTHR

1 Headquarters, U.S. Army Material Command
Research Division, R & D Directorate
Washington 25, D. C.
Attn: Physics & Electronics Branch
Electronics Section

1 Commanding Officer
Diamond Ordnance Fuze Laboratories
Washington 25, D. C.
Attn: Librarian, Room 211, Bldg. 92

1 Operations Evaluation Group
Office of the CNO (Op03EG)
Navy Department
Washington 25, D. C.

1 Chief of Naval Operations
Tech. Analysis & Advisory Group (OP-07T)
Pentagon
Washington 25, D. C.

1 Commanding Officer
U.S. Army Personnel Research Office
Washington 25, D. C.

1 Commanding Officer & Director
David W. Taylor Model Basin
Navy Department
Washington 7, D. C.
Attn: Code 142, Library

1 Bureau of Ships
Department of the Navy
Washington 25, D. C.
Attn: Code 686

1 Bureau of Ships
Navy Department
Washington 25, D. C.
Attn: Code 732

1 Technical Library, DLI-3
Bureau of Naval Weapons
Department of the Navy
Washington 25, D. C.

1 Director
Naval Research Laboratory
Washington 25, D. C.
Attn: Code 5140

1 Department of the Navy
Office of Naval Research
Washington 25, D. C.
Attn: Code 437

1 Dr. H. Wallace Sinaiko
Institute for Defense Analyses
Research & Engineering Support Division
1666 Connecticut Ave., N.W.
Washington 9, D. C.

1 Data Processing Systems Division
National Bureau of Standards
Conn. at Van Ness
Room 239, Bldg. 10
Washington 25, D. C.
Attn: A. K. Smilow

1 Exchange and Gift Division
The Library of Congress
Washington 25, D. C.

1 NASA Headquarters
Office of Applications
400 Maryland Avenue, S.W.
Washington 25, D. C.
Attn: Mr. A. M. Greg Andrus
Code FC

1 AOGC (PGAPI)
Eglin Air Force Base
Florida

1 Commanding Officer
Office of Naval Research, Chicago Branch
6th Floor, 230 North Michigan
Chicago 1, Illinois

1 Laboratories for Applied Sciences
University of Chicago
6220 South Drexel
Chicago 37, Illinois

1 Librarian
School of Electrical Engineering
Purdue University
Lafayette, Indiana

1 Commanding Officer
U.S. Army Medical Research Laboratory
Fort Knox, Kentucky

2 Keats A. Pullen, Jr.
Ballistic Research Laboratories
Aberdeen Proving Ground, Maryland

1 Commander
Air Force Cambridge Research Laboratories
Laurence G. Hanscom Field
Bedford, Massachusetts
Attn: CRXL

1 Director
U.S. Army Human Engineering Laboratories
Aberdeen Proving Ground, Maryland

5 Scientific & Technical Information Facility
P. O. Box 5700
Bethesda, Maryland
Attn: NASA Representative (S-AK/DL)

1 Mr. James Tippett
National Security Agency
Fort Meade, Maryland

1 Dr. Lloyd Hollingsworth
Director, ERD
AFCRL
L. G. Hanscom Field
Bedford, Massachusetts

1 Major William Harris
Electronics Systems Division
L. G. Hanscom Field
Bedford, Massachusetts

1 Instrumentation Laboratory
Massachusetts Institute of Technology
68 Albany Street
Cambridge 39, Massachusetts
Attn: Library W1-109

1 Research Laboratory of Electronics
Massachusetts Institute of Technology
Cambridge 39, Massachusetts
Attn: Document Room 26-327

1 Dr. Robert Kingston
Lincoln Laboratories
Lexington, Massachusetts

1 Lincoln Laboratory
Massachusetts Institute of Technology
P. O. Box 73
Lexington 73, Massachusetts
Attn: Library, A-082

1 Sylvania Electric Products Inc.
Electronic Systems
Waltham Labs. Library
100 First Avenue
Waltham 54, Massachusetts

1 Minneapolis-Honeywell Regulator Co.
Aeronautical Division
2600 Ridgeway Road
Minneapolis 13, Minnesota
Attn: Mr. D. F. Elwell
Main Station: 625

1 Inspector of Naval Material
Bureau of Ships Technical Representative
1902 West Minnehaha Avenue
St. Paul 4, Minnesota

20 Activity Supply Officer, USAELRDL
Building 2504, Charles Wood Area
Fort Monmouth, New Jersey
For: Accountable Property Officer
Marked: For Inst. for Exploratory Research
Inspect at Destination
Order No. 5776-PM-63-91

1 Commanding General
U.S. Army Electronic Command
Fort Monmouth, New Jersey
Attn: AMSEL-RE

1 Mr. A. A. Lundstrom
Bell Telephone Laboratories
Room 2E-127
Whippany Road
Whippany, New Jersey

1 AFMDC (MDSGP/Capt. Wright)
Holloman Air Force Base
New Mexico

1 Commanding General
White Sands Missile Range
New Mexico

1 Microwave Research Institute
Polytechnic Institute of Brooklyn
55 John Street
Brooklyn 1, New York

1 Cornell Aeronautical Laboratory, Inc.
4455 Genesee Street
Buffalo 21, New York
Attn: J. P. Desmond, Librarian

1 Sperry Gyroscope Company
Marine Division Library
155 Glen Cove Road
Carle Place, L.I., New York
Attn: Mrs. Barbara Judd

1 Rome Air Development Center
Griffiss Air Force Base
New York
Atten: Documents Library
RAALD

1 Library
Light Military Electronics Department
General Electric Company
Armament & Control Products Section
Johnson City, New York

1 Columbia Radiation Laboratory
Columbia University
538 West 120th Street
New York 57, New York

1 Mr. Alan Barnum
Rome Air Development Center
Griffiss Air Force Base
Rome, New York

1 Dr. E. Howard Holt
Director
Plasma Research Laboratory
Rensselaer Polytechnic Institute
Troy, New York

3 Commanding Officer
U.S. Army Research Office (Durham)
Box CM, Duke Station
Durham, North Carolina
Attn: CRD-AA-IP, Mr. Ulsh

1 Battelle-DEFENDER
Battelle Memorial Institute
505 King Avenue
Columbus 1, Ohio

1 Aeronautical Systems Division
Navigation and Guidance Laboratory
Wright-Patterson Air Force Base
Ohio

1 Aeronautical Systems Division
Directorate of Systems Dynamic Analysis
Wright-Patterson Air Force Base
Ohio

1 Commanding Officer (AD-5)
U.S. Naval Air Development Center
Johnsville, Pennsylvania
Attn: NADC Library

2 Commanding Officer
Frankford Arsenal
Philadelphia 37, Pennsylvania
Attn: SMUFA-1300

1 H. E. Cochran
Oak Ridge National Laboratory
P. O. Box X
Oak Ridge, Tennessee

1 U.S. Atomic Energy Commission
Office of Technical Information Extension
P. O. Box 62
Oak Ridge, Tennessee

1 President
U.S. Army Air Defense Board
Fort Bliss, Texas

1 U.S. Air Force Security Service
San Antonio, Texas
Attn: ODC-R

1 Director
Human Resources Research Office
The George Washington University
300 North Washington Street
Alexandria, Virginia

20 ASTIA Technical Library AFL 2824
Arlington Hall Station
Arlington 12, Virginia
Attn: TISLL

1 Commander
U.S. Army Research Office
Highland Building
3045 Columbia Pike
Arlington 4, Virginia

1 U.S. Naval Weapons Laboratory
Computation and Analysis Laboratory
Dahlgren, Virginia
Attn: Mr. Ralph A. Niemann

2 Army Material Command
Research Division
R & D Directorate
Bldg. T-7
Gravelley Point, Virginia